UNIVERSITY OF SCIENCE AND TECHNOLOGY OF HANOI
DEPARTMENT OF SPACE AND APPLICATIONS

Master in Space: Earth Observation, Astrophysics, Satellite Technology

FINAL REPORT

Student name: Dao Duc Trung
Intake: 2024
Academic year: 2024-2025

PERFORMANCE EVALUATION FOR THE BELLE II CENTRAL DRIFT CHAMBER AFTER LONG-SHUTDOWN-I USING 2024 DATA

Supervisor: Dr. *Nguyen Anh Kỳ*

July 30, 2025

Abstract

The Belle II experiment at the SuperKEKB electron–positron collider in Tsukuba, Japan, is designed to probe the frontiers of particle physics by studying CP violation, rare B meson decays, exotic hadron states, and other potential signs of new physics beyond the Standard Model. With an unprecedented integrated luminosity target of 50 ab^{-1}, Belle II requires extremely precise charged-particle tracking and momentum resolution in order to fully exploit the physics opportunities offered by high-intensity e^+e^- collisions. Central to this capability is the Central Drift Chamber (CDC), which provides high-granularity measurements of charged-particle trajectories, transverse and longitudinal impact parameters, and contributes critically to vertex reconstruction.

During Long Shutdown I (LS1), the CDC underwent a series of important maintenance and upgrade activities to address performance challenges observed during earlier phases of operation. These challenges included gas contamination in the detector volume, aging effects on sensing wires, and instabilities in the front-end electronics, all of which contributed to degraded tracking performance. Upgrades included the installation of oxygen removal systems with Nafion dryer and platinum catalyst, enhancements to gas circulation and monitoring infrastructure, and careful reconditioning of sensitive wire and readout components. These interventions were aimed at ensuring the long-term stability and optimal functionality of the CDC under the demanding conditions of the high-luminosity Belle II program.

This report presents a detailed performance evaluation of the Belle II CDC using cosmic-ray and 2024 collision data collected after LS1. A split-track method was employed, in which tracks are divided into upper and lower segments, and differences in key track parameters are used to extract single-track resolutions. The analysis covers transverse impact parameter (d_0), longitudinal impact parameter (z_0), azimuthal angle (ϕ_0), dip angle ($\tan\lambda$), and transverse momentum (p_t). The results show significant improvements compared to pre-LS1 performance, with impact parameter resolutions improving by 20–25% and transverse momentum resolution reaching ~0.9%. These improvements confirm that the CDC has successfully recovered and even exceeded its design performance, ensuring that Belle II is fully prepared for its core physics program—precision CP violation measurements and searches for rare phenomena.

Table of Contents

FINAL REPORT

UNIVERSITY OF SCIENCE AND TECHNOLOGY OF HANOI
DEPARTMENT OF SPACE AND APPLICATIONS

Performance Evaluation for The Belle II Central Drift Chamber after Long-Shutdown-I Using 2024 Data

By: Dao Duc Trung
July 30, 2025

---

1. Introduction

1.1 Belle II Overview and Physical Motivation

The study of **electron–positron (e^+e^-) collisions** provides one of the cleanest and most controlled environments for exploring the fundamental interactions of matter. When an electron and a positron collide at high energy, they annihilate and convert their entire energy into new particles. This process proceeds primarily through the exchange of a virtual photon or Z boson, producing quark–antiquark or lepton–antilepton pairs, and, at certain energies, resonant states such as the Υ family. By tuning the beam energy precisely to the **Υ(4S) resonance (10.58 GeV)**, the collision final state predominantly consists of pairs of B mesons. This makes e^+e^- colliders uniquely suited for studying the properties of heavy flavor physics, particularly B meson decays.

The **Belle II experiment**, located at the SuperKEKB accelerator in Tsukuba, Japan, was designed to exploit this opportunity. Its ultimate scientific goal is to test the limits of the **Standard Model (SM)** and to search for evidence of **new physics**. Belle II focuses on measuring **CP violation** in the B meson system with unprecedented precision, thereby deepening our understanding of the matter–antimatter asymmetry of the universe. In addition, it searches for **rare and forbidden decays**, probes **lepton flavor universality** by comparing the behavior of electrons, muons, and taus, and investigates the structure of **exotic hadrons** such as tetraquarks and pentaquarks. The experiment also provides sensitivity to new particles predicted in **dark sector models**, such as dark photons or other weakly interacting light states. Together, these studies allow Belle II to complement discoveries at hadron colliders: while the LHC probes the highest energy scales, Belle II excels in precision and sensitivity to subtle deviations from the SM.

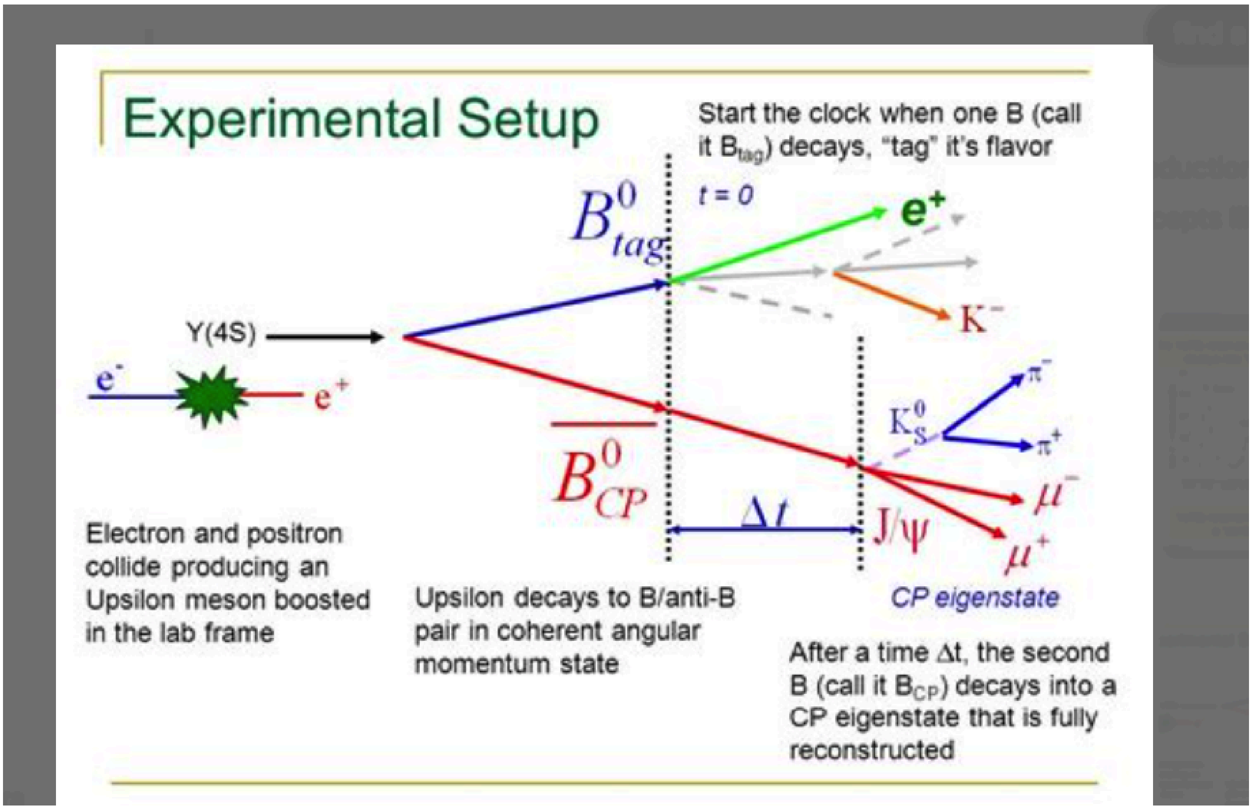

Figure 1.1: Schematic of Belle II CP violation method (source: Belle Collaboration).

An electron and positron collide to form an Y(4S) meson, which decays into a coherent B–anti-B meson pair. One meson (B_tag) decays at time *t = 0* and is used for flavor tagging, while the other (B_CP) decays after a time difference Δt into a CP eigenstate such as $J/\psi K\_S^0$. By comparing the decay times and final states of the two mesons, time-dependent CP violation parameters can be extracted. This is the core methodology of Belle II's CP violation program. (Adapted from Belle Collaboration / standard Belle II CPV illustrations)

The **SuperKEKB collider** employs an innovative "nano-beam" scheme that compresses the electron and positron beams to nanometer dimensions at the interaction point, achieving luminosities about forty times greater than its predecessor, KEKB. At its design luminosity, SuperKEKB aims to deliver an integrated dataset of **50 ab^{-1}**, enabling Belle II to become the world's leading precision flavor experiment. Surrounding the collision point, the **Belle II detector** is a large-scale spectrometer composed of several subdetectors, including the vertex detector (VXD), the central drift chamber (CDC), particle identification devices, the electromagnetic calorimeter, and the outer muon/KL system. These systems work in synergy to reconstruct final states with high precision and efficiency.

The **Central Drift Chamber (CDC)** is the largest tracking subsystem in Belle II and plays a central role in reconstructing charged-particle trajectories. It is a cylindrical detector filled with a helium–ethane gas mixture and contains thousands of precisely aligned sense and field wires. As charged particles traverse the chamber, they ionize the gas, and the freed electrons drift to the sense wires under an electric field, where the signals are read out. From these signals, the CDC reconstructs particle trajectories and provides several key measurements. It determines the **momentum** of charged particles from their curvature in the 1.5 T solenoidal magnetic field; it measures the **impact parameters** d_0 and z_0, which describe the closest approach of the track to the beamline and are vital for vertex reconstruction; it records the **track angles** ϕ_0 and tan λ, which define the azimuthal and polar orientation of the particle's path; and it provides **dE/dx information** on energy loss, which contributes to particle identification. Because of this broad functionality, the CDC directly influences Belle II's ability to achieve its core physics goals.

During the initial operation of Belle II between 2019 and 2022, however, the CDC faced several challenges. **Gas contamination** from oxygen and moisture degraded the drift properties of the chamber,

wire aging reduced signal quality, and **instabilities in the front-end electronics** caused calibration drifts. Together, these issues resulted in performance degradation, with impact parameter and momentum resolutions falling below their design levels. Such limitations, if not corrected, would have significantly reduced Belle II's capacity to achieve its intended precision physics program.

To restore and secure the detector's performance, a program of targeted upgrades and maintenance was carried out during **Long Shutdown I (LS1, 2022–2023)**. A Nafion dryer and platinum catalyst were installed to continuously remove oxygen and moisture from the gas mixture, additional sensors were deployed to monitor gas purity in real time, and sense wires were reconditioned to mitigate aging effects. The front-end readout electronics were also updated and recalibrated to improve stability. These interventions were designed not only to recover lost performance but also to ensure long-term sustainability of the CDC under the high-luminosity conditions expected as SuperKEKB progresses toward its design goals.

This report presents a **comprehensive performance evaluation of the CDC after LS1**, based on cosmic-ray and 2024 collision data. The evaluation uses the **split-track method**, in which tracks are divided into upper and lower halves and the differences in reconstructed parameters are analyzed to extract single-track resolutions. The study focuses on five principal tracking parameters: the transverse impact parameter (d_0), the longitudinal impact parameter (z_0), the azimuthal angle (ϕ_0), the dip angle ($\tan\lambda$), and the transverse momentum (p_t). By comparing the post-LS1 results with those obtained before LS1, this analysis quantifies the improvements achieved through the upgrades and confirms the CDC's readiness to support Belle II's demanding physics program.

1.2 Purpose of Evaluation

This report focuses on checking how well the Central Drift Chamber (CDC) — Belle II's main tracking device — is performing after a major maintenance period known as the first Long Shutdown (LS1). LS1 took place from July 2022 to December 2023. During this time, engineers and scientists worked on important upgrades, especially to the CDC's gas system, which is crucial for its accuracy.

The evaluation compares two sets of data:

- **Before LS1:** Data from 2022, when the CDC was already showing signs of reduced performance.
- **After LS1:** New data collected in 2024, after the upgrades were completed.

By comparing these results, we aim to see how much the CDC's performance has improved and whether the upgrades — particularly the gas system improvements — solved the issues seen before LS1.

1.3 CDC Performance Issues

Prior to Long-Shutdown-I (LS1), the Belle II Central Drift Chamber (CDC) experienced progressive and measurable performance degradation. This decline was most pronounced in the final data-taking periods of 2022 and was traced primarily to instability in the CDC gas system (Belle II Collaboration, 2022). Contamination from oxygen (O_2) and water vapor (H_2O) adversely affected both the spatial resolution and tracking accuracy of the detector (Status of CDC, 2024).

Oxygen contamination reduced electron drift velocity and increased electron–ion recombination, while water vapor introduced fluctuations in gas gain. Together, these effects compromised uniformity in drift properties, leading to degraded hit localization and track fitting precision (Taniguchi et al., 2017). The situation was exacerbated by failures in the gas quality monitoring sensors — specifically O_2 and dew-point sensors — which prevented timely identification and correction of the problem (KEK IPNS, 2016). As a result, CDC performance continued to worsen throughout the final 2022 runs (Belle II CDC Group, 2021).

This degradation is clearly illustrated in **Figure 1**, which plots the resolution (σ_{68}) of key track parameters against **bucket number**, where each bucket corresponds to a sequential data-taking period:

1. **Top-left: d_0 resolution (μm)**
    - **Definition:** The transverse impact parameter — the shortest distance in the x–y plane between the reconstructed track and the beam axis.
    - **Trend:** Resolution worsens from ~238 μm in bucket 34 to over 270 μm in bucket 36.
    - **Impact:** Reduces transverse vertex reconstruction accuracy, affecting analyses involving displaced vertices (Belle II Collaboration, 2022).
2. **Top-right: z_0 resolution (μm)**
    - **Definition:** The longitudinal impact parameter — the distance along the beam axis from the point of closest approach to the interaction point.
    - **Trend:** Increases from ~0.270 mm to ~0.300 mm.
    - **Impact:** Reduces the precision of locating particle origins along the beam axis (Belle II CDC Group, 2021).
3. **Middle-left: ϕ_0 resolution (°)**
    - **Definition:** The azimuthal angle at the point of closest approach.
    - **Trend:** Degrades from ~0.080° to ~0.087° (~9% loss in angular precision).
    - **Impact:** Reduces accuracy in reconstructing track direction in the transverse plane (Belle II Collaboration, 2022).
4. **Middle-right: tanλ resolution (%)**
    - **Definition:** Dip angle, related to the slope of the track in the r–z plane.
    - **Trend:** Increases from ~0.00475% to ~0.0053%.
    - **Impact:** Reduces precision in determining the particle's inclination relative to the beam axis (Belle II CDC Group, 2021).
5. **Bottom: Pt resolution (%)**
    - **Definition:** Resolution of transverse momentum measurement.
    - **Trend:** Worsens from ~2.35% to ~2.56%.
    - **Impact:** Decreases accuracy in momentum determination, affecting mass reconstruction and kinematic measurements.

Overall Interpretation:
The consistent upward trends across all parameters indicate a **system-wide degradation** rather than isolated component issues. Gas contamination was the dominant factor, as it affects drift velocity stability, gas gain uniformity, and the precision of both spatial and angular measurements (Status of CDC, 2024). The clear worsening over buckets provided strong justification for the **comprehensive gas system overhaul during LS1**, which included:

- Installation of **Nafion dryers** to control humidity.

- **Pt-catalyst oxygen filters** to remove O_2 contamination.
- **Dual high-accuracy O_2 and dew-point sensors** for continuous monitoring.
- **Quick calibration lines** for maintaining sensor accuracy.

These interventions were aimed at restoring and stabilizing CDC performance for the post-LS1 data-taking period (Status of CDC, 2024).

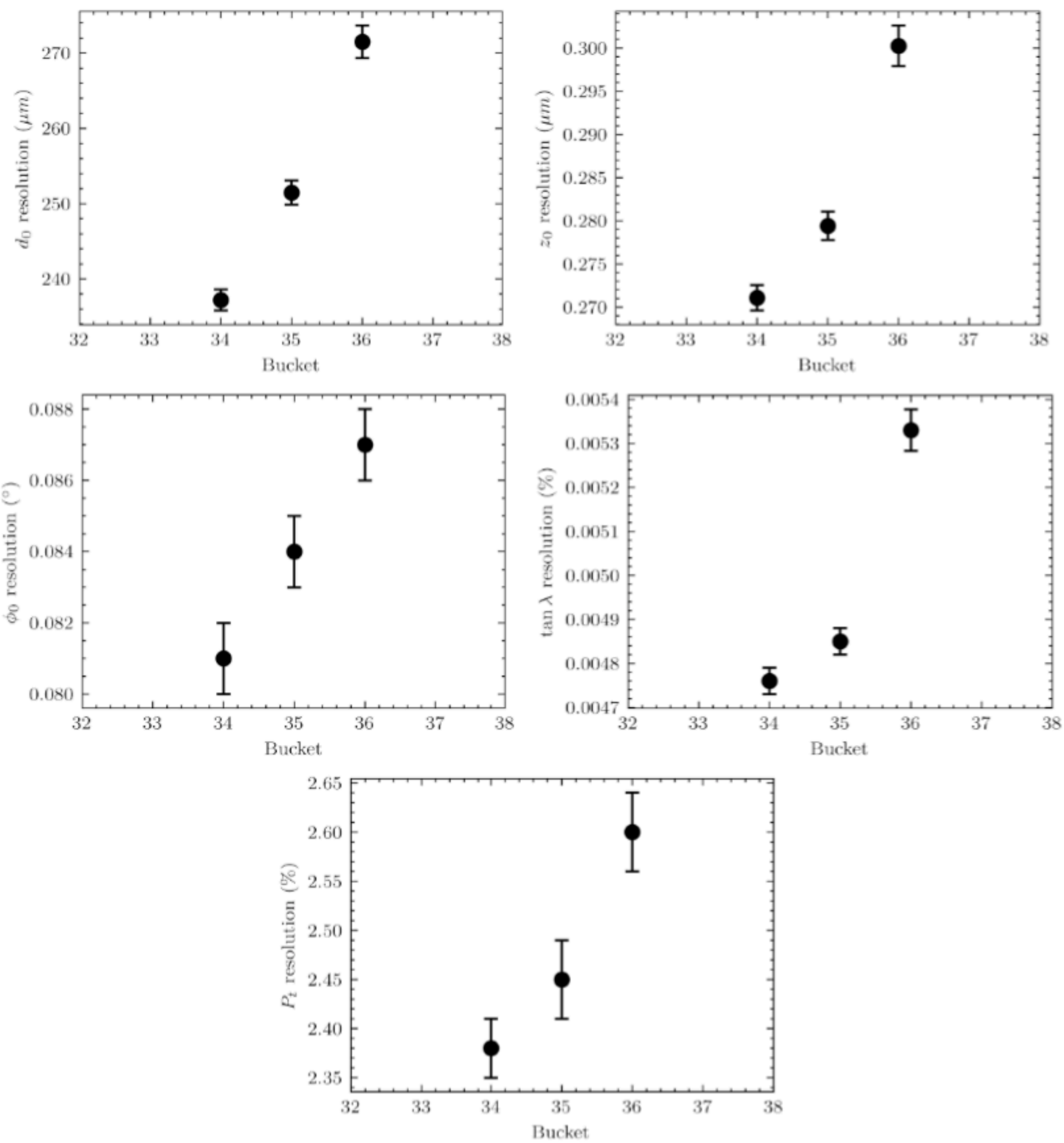

Figure 1.3: CDC performance before LS1, showing degradation in key track parameter resolutions (d_0, z_0, ϕ_0, tanλ, Pt) across the final 2022 data-taking buckets. Adapted from Tran Hoang Viet's thesis (Tran, H. V. 2023).

2. Belle II Experimental Setup

2.1 Overview of the SuperKEKB Accelerator

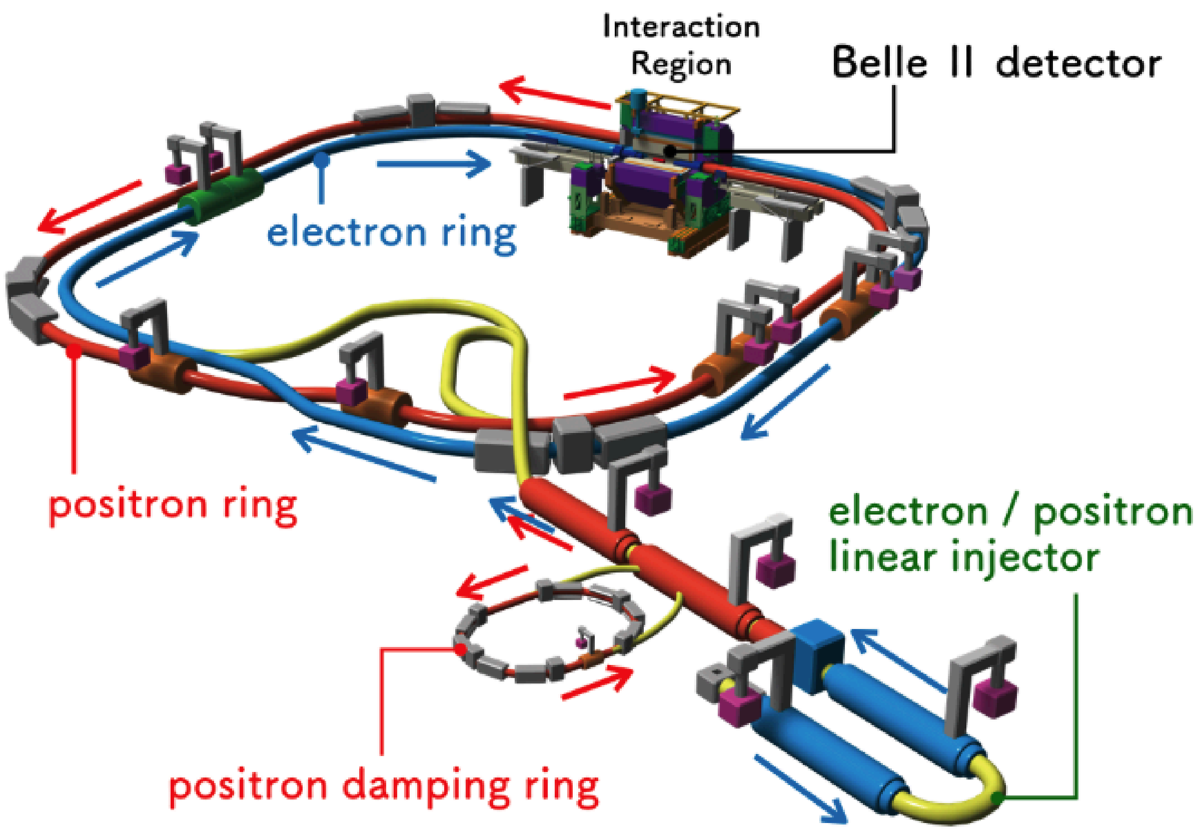

Figure 2.1: Layout of the SuperKEKB accelerator complex

- **Electron/Positron Linear Injector**

At the start of the acceleration chain, the **linear accelerator (Linac)** produces high-energy beams of electrons and positrons.

- Electrons are generated directly and accelerated to 7 GeV.
- Positrons are created by directing high-energy electrons onto a conversion target, producing electron–positron pairs. The positrons are captured and further accelerated before injection.

- **Positron Damping Ring**

Freshly produced positrons have large transverse emittance (beam spread). They are therefore injected into a **damping ring**, where synchrotron radiation reduces their emittance and makes the beam narrower and more stable. After damping, the positrons are reinjected into the main collider ring for collisions.

- **Dual Storage Rings (Electron and Positron Rings)**

SuperKEKB employs two concentric storage rings, each about **3.0 km in circumference**:

- The **High Energy Ring (HER)** for **7 GeV electrons** (blue in the diagram).

- The **Low Energy Ring (LER)** for **4 GeV positrons** (red in the diagram).

The two beams circulate in opposite directions and are brought to collide at the **interaction region**.

- **Interaction Region and the Belle II Detector**

The collision point of the two beams is located inside the **Belle II detector**. This is where electron–positron annihilation produces the ϒ(4S) resonance, which subsequently decays into pairs of B mesons. The Belle II detector surrounds this region and records all final-state particles from the collisions.

- **Nano-Beam Scheme and High Luminosity**

SuperKEKB achieves its record luminosity (goal: $\mathbf{8 \times 10^{35}\ cm^{-2}\ s^{-1}}$) through the **nano-beam scheme**, which squeezes the transverse size of the beams at the interaction point to nanometer scales. This increases the overlap of the colliding beams and maximizes collision probability.

- The asymmetric beam energies (7 GeV electrons vs. 4 GeV positrons) impart a **Lorentz boost** to the ϒ(4S) system, which is crucial for measuring **time-dependent CP violation** in B mesons.

2.2 Belle II Detector Structure

The Belle II detector is a **general-purpose spectrometer** placed at the interaction point of the SuperKEKB collider. It has a **cylindrical, layered design** that enables precise detection, identification, and measurement of particles produced in high-energy electron–positron collisions (Abe et al., 2013; Belle II Collaboration, n.d.).

Sub-Detector Components (Innermost to Outermost):

1. **Vertex Detector (VXD)**
    - **Pixel Detector (PXD):** Two innermost layers using DEPFET pixel sensors, positioned just 14 mm and 22 mm from the beamline. Offers extremely high spatial resolution (~25 µm), ideal for pinpointing particle decay vertices (Barth et al., 2016)
    - **Silicon Vertex Detector (SVD):** Surrounds the PXD with four double-sided silicon strip layers, extending the tracking coverage and improving reconstruction efficiency (Friedl et al., 2016).

2. **Central Drift Chamber (CDC)**
    - The primary tracking detector, filled with a 50% He–50% C_2H_6 gas mixture. It uses fine cells and fast electronics to reconstruct charged-particle trajectories and measure momenta within the 1.5 T magnetic field (Taniguchi et al., 2017; Svidras, 2020).

3. **Particle Identification (PID) Systems**
    - **Time-of-Propagation (TOP) Counter:** Located in the barrel region; employs Cherenkov light generated in quartz bars and precise timing to discriminate between particle species like pions and kaons (Nishida et al., 2017).

    - **Aerogel Ring Imaging Cherenkov (ARICH) Detector:** Positioned in the forward end-cap; uses aerogel to produce Cherenkov radiation for complementary PID performance (Iijima et al., 2017)

4. **Electromagnetic Calorimeter (ECL)**
    - Consists of CsI(Tl) crystals in the barrel (and pure CsI crystals in the end-caps),

measuring the energy of photons and neutral particles with high precision. The system supports waveform sampling readout techniques (Won et al., 2018; Wikipedia, 2025).

5. **K_L⁰ and Muon Detector (KLM)**

   ○ Surrounds the outer radius of the detector and is embedded in the iron flux return. It uses Resistive Plate Chambers (barrel) and scintillator/WLSF with SiPMs (end-caps) to identify muons and detect long-lived neutral kaons (Adachi et al., 2018; Wikipedia, 2025).

Integrated Functionality

- **Vertex detection (PXD + SVD):** Locates decay points of heavy particles like B and D mesons with high precision.

- **Tracking & momentum measurement (CDC):** Captures the curvature of charged particles in the magnetic field, delivering accurate momentum information.

- **Particle Identification (TOP + ARICH):** Differentiates between particle types, enriching physics analyses such as CP violation and rare decay studies.

- **Energy measurement (ECL):** Detects photons and neutral particles, vital for reconstructing events like π^0 decays, and contributes to overall calorimetric data collection.

- **Outer detection (KLM):** Identifies muons and neutral kaons, completing the event picture and supporting both charged and neutral particle detection.

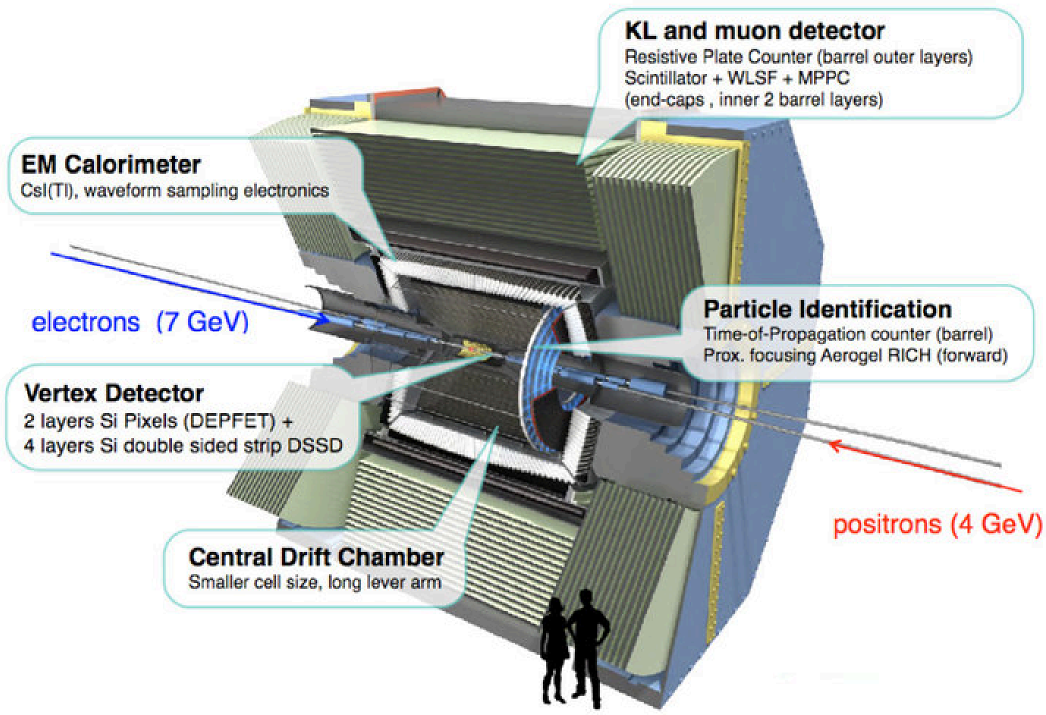

Figure 2.2: Schematic cross-section of the Belle II detector, showing all main sub-detector systems

Vertex Detector (PXD + SVD), Central Drift Chamber (CDC), PID systems (TOP barrel, ARICH forward), Electromagnetic Calorimeter (ECL), and K_L⁰/Muon Detector (KLM) outside the solenoid.

This layered configuration ensures accurate tracking, energy measurement, and particle identification (Belle II Collaboration, n.d.).

2.3 Central Drift Chamber (CDC)

The **Central Drift Chamber (CDC)** is Belle II's principal tracking detector—a large, cylindrical wire chamber that plays several critical functions:

- **Charged-particle tracking**: Reconstructs the paths of particles within the 1.5 T magnetic field.
- **Momentum measurement**: Determines momentum by analyzing the curvature of tracks.
- **Particle identification (PID)**: Estimates particle type using energy loss (dE/dx) in gas.
- **Trigger contribution**: Supplies fast signals essential for event selection (Taniguchi et al., 2017)

2.3.1. CDC structure

For the Belle II Central Drift Chamber (CDC), the radial coverage of the active sensing elements extends from a minimum of 168 mm to a maximum of 1,111.4 mm, as determined by the radius of the innermost and outermost sense wires, respectively (Abe et al., 2010). This represents a significant expansion compared to the Belle I CDC, which covered radial positions between 88 mm and 863 mm (Abe et al., 2010). The increased radial span in Belle II enhances the tracking lever arm, thereby improving momentum resolution and overall tracking performance. Compared to Belle I's 50 layers, Bella II upgraded to 56 layers, thanks to the substitution of inner regions with a silicon tracker. To reduce occupancy in the high-luminosity environment, small drift cells (~2.5 mm size) were adopted, increasing the sense wire count from approximately 8,000 to around 15,000 (Abe et al., 2013). The CDC uses 30 µm gold-plated tungsten sense wires surrounded by 126 µm aluminum field wires

2.3.2. Gas System and Drift Mechanism

The chamber is filled with a **50:50 helium–ethane (He:C_2H_6) gas mixture**, chosen for its long radiation length, fast drift velocity (~3.3 cm/µs), and suitability for dE/dx measurement (Taniguchi et al., 2017; Status of CDC, 2024)

A charged particle passing through the CDC ionizes the gas, generating electron–ion pairs. Electrons drift toward the **anode (sense) wires**, initiating an avalanche as they approach. The **drift time**—the time taken for electrons to reach wires—is recorded and used to pinpoint the particle's trajectory with **~100 µm spatial resolution** (Indico Belle II, 2019). **2.3.3 Front-End Readout Electronics**

The Belle II CDC uses a new front-end electronics system designed to handle the much higher collision rates at SuperKEKB. The new system works faster and can process signals even when background noise is high. It includes both **time-to-digital converters (TDCs)** to measure drift times and **analog-to-digital converters (ADCs)** to measure signal charge. (Abe et al., 2010)

2.3.3. Hit Rate and Occupancy

Anticipated hit rates per layer are as high as **100 kHz** (scaled from 5 kHz currently) during operation—an increase by a factor of 20. **Drift times** across the cell range from **80–300 ns**, depending on radius and field strength. Therefore, expected **occupancy** per cell can reach 1–3% (calculated as 100 kHz × 80–300 ns = 0.01–0.03), which remains manageable for high trigger efficiency (Svidras, 2020).

2.3.4. Momentum Resolution

With the combined tracking performance of the **Silicon Vertex Detector (SVD)** and the CDC, a

momentum resolution of the form $\sigma_{pt}/\ p_t \approx$ (0.11–0.19)% ⊕ 0.30% is achievable—demonstrating high-precision momentum reconstruction capabilities (Abe et al., 2013; Belle II Collaboration, 2022).

Summary of Key Performance Features

Feature	Specification	Purpose & Benefit
Layer Coverage	168 – 1,111.4 mm (radial), 56 layers	Maximizes tracking volume and resolution
Cell Size	~2.5 mm	Keeps occupancy low even under high hit rates
Hit Rate	Up to 100 kHz	Ensures accuracy during intense collision rate periods
Occupancy	1–3%	Maintains tracking precision despite background
Readout	Fast FADC	Rapid digitization for clear signal amidst noise
Momentum Resolution	~0.11–0.19% ⊕ 0.30%/β	Combines SVD + CDC for high-precision momentum measurement

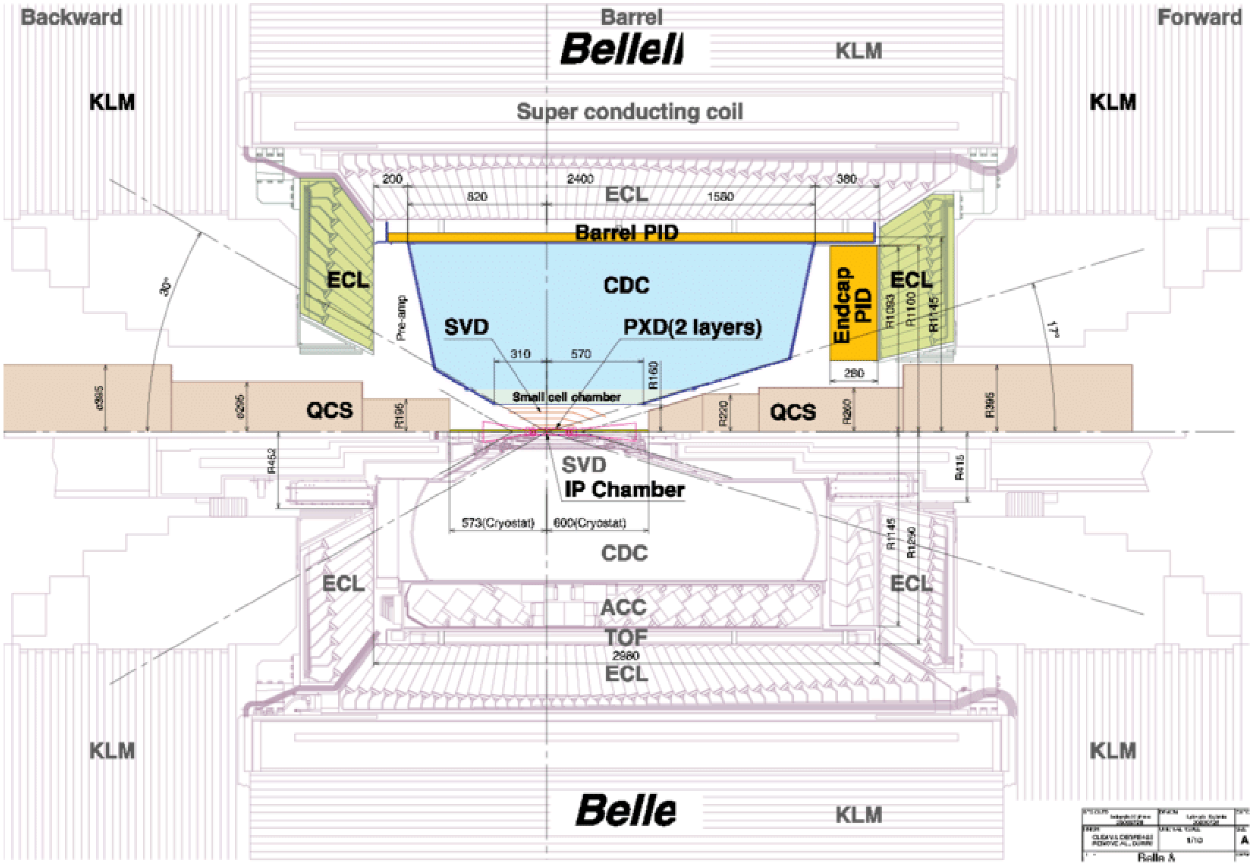

Figure 2.3.1: Cross-section of the Belle II detector

Horizontal cross-section of the Belle II detector, highlighting the CDC's location relative to neighboring subsystems (PXD, TOP, ECL).

The figure shows a longitudinal cross-section of the **Belle II detector** at the SuperKEKB interaction point, with each subsystem arranged concentrically around the beam line. At the very center, the electron and positron beams collide inside the interaction point chamber, which is surrounded by the **Pixel Detector (PXD)** and the **Silicon Vertex Detector (SVD)**. These two systems provide ultra-precise spatial measurements that allow reconstruction of decay vertices from short-lived particles such as B and D mesons. Encasing the vertex detectors is the **Central Drift Chamber (CDC)**, shown as the large blue region, which is filled with a helium–ethane gas mixture and instrumented with thousands of sense wires. As charged particles traverse this volume, the CDC measures their curvature in the 1.5 T solenoidal magnetic field and provides precise determinations of momenta, impact parameters, and track angles.

Surrounding the CDC are the **particle identification systems**, composed of the Time-of-Propagation (TOP) counter in the barrel and the Aerogel Ring Imaging Cherenkov (ARICH) detector in the forward endcap. These devices measure Cherenkov light and timing information to distinguish between pions, kaons, and protons with high efficiency, which is critical for flavor physics analyses. Outside the PID systems lies the **Electromagnetic Calorimeter (ECL)**, built from thallium-doped cesium iodide crystals, which absorbs photons and electrons and measures their energies and shower profiles. Encasing all of these subsystems is a large **superconducting solenoid coil**, which generates the 1.5 T magnetic field used for tracking.

Finally, the outermost system is the **KLM detector**, embedded in the iron flux return of the magnet. It identifies muons and long-lived neutral kaons, thereby completing the overall event reconstruction. Also visible in the cross-section are the **QCS final-focus quadrupole magnets**, which squeeze the beams to nanometer sizes at the interaction point, enabling the nano-beam scheme that gives SuperKEKB its world-record luminosity. Together, these subsystems form a highly integrated spectrometer: tracks born at the interaction point pass sequentially through the PXD and SVD, the CDC, the PID layers, the calorimeter, and finally the muon system. Each layer contributes complementary information that allows Belle II to fully reconstruct the final states of e^+e^- collisions at the Υ(4S), with the CDC playing the central role in tracking performance.

2.4 CDC Operational Challenges Before LS1

Before Long-Shutdown-I (LS1, July 2022–December 2023), the CDC encountered operational challenges related to gas purity. Specifically, contamination from oxygen (O_2), water vapor (H_2O), and hydrogen (H_2) had increased significantly due to sensor failures in the gas monitoring system. The degraded gas conditions negatively impacted drift velocity uniformity and reduced the gas amplification factor, thereby worsening spatial resolution and overall tracking performance. Addressing these issues was a key motivation behind performing comprehensive maintenance and upgrading of the CDC gas system during LS1.

---

3. Long-Shutdown-I (LS1): Upgrades and Maintenance

3.1 Motivation and Need for LS1

The Belle II experiment ran continuously from early 2019 until mid-2022. During that time, it reached many of its scientific goals and collected a very large amount of collision data. However, running the detector for several years without a long break caused wear and tear on its components (x).

One of the systems most affected was the **Central Drift Chamber (CDC)**, which is Belle II's main device for tracking charged particles. Several problems gradually reduced its performance:

- **Gas contamination** inside the CDC
- **Aging of the sensing wires**
- **Loss of gas purity** over time

These issues hurt the detector's ability to measure particle tracks accurately. In particular, two important measurements — the **longitudinal impact parameter** (z_0) and the **transverse impact parameter** (d_0) — became less precise (Belle II CDC Group, 2021).

Investigations showed that the main reason for this drop in performance was **unstable gas conditions**. The gas inside the CDC must be kept extremely clean and at the right composition, but **oxygen (O_2)** and **water vapor (H_2O)** had built up. This happened because the sensors used to monitor gas quality — especially the O_2 and humidity sensors — were failing. Without reliable monitoring, the contamination was not detected early enough, and the problem got worse over time (Status of CDC, 2024).

To fix these problems and make sure Belle II could continue producing accurate physics results, the team scheduled a **Long Shutdown-I (LS1)** from **July 2022 to December 2023**. This was a planned, extended maintenance period to:

- Fully restore and stabilize the CDC's gas system
- Replace or repair damaged and outdated equipment
- Upgrade detector components to handle the high-luminosity conditions expected in future runs
- Improve the overall tracking precision and reliability of the detector

In short, LS1 was not just routine maintenance — it was essential for bringing the detector back to top performance and ensuring that future data would be as precise and trustworthy as possible (KEK IPNS, 2016).

3.2 Detailed List of CDC Upgrades During LS1

To fix the gas problems and bring the Central Drift Chamber (CDC) back to full performance, Belle II carried out a set of major upgrades during **Long Shutdown-I (LS1)**. These upgrades focused on keeping the drift gas clean, stable, and well-monitored at all times. Figure below shows the upgraded CDC gas system layout after LS1 (Status of CDC, 2024).

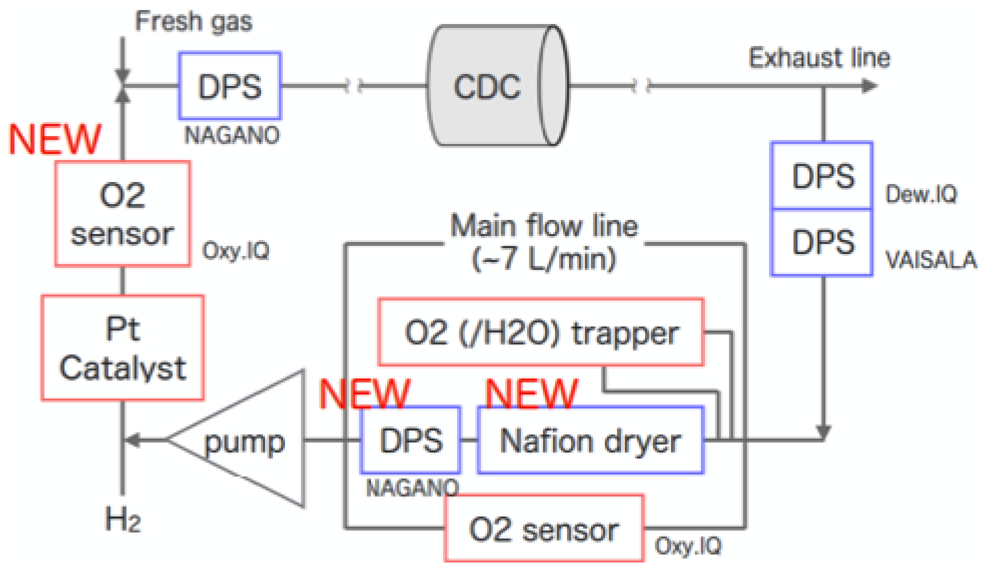

Figure 3.2: System layout of CDC

Flow Lines

- The gas system supplies **fresh gas** to the CDC and recirculates it through purification and monitoring components.
- **Dryer line**: Uses a **Nafion dryer/humidifier** to control moisture levels in the gas. Sometimes combined with an **O_2/H_2O trapper** to remove oxygen and water vapor impurities.
- Flow rate through the **main flow line** is about **7 L/min** (Status of CDC, 2024).

Oxygen (O_2) Control

- **O_2 sensors** are placed **before and after** the **O_2 filter** (Pt catalyst). The **Pt catalyst** removes oxygen from the gas stream.
- The O_2 sensors allow precise measurement of oxygen levels, so the efficiency of the filter can be monitored in real-time.
- **New lines** have been added for **quick calibration** of these sensors without interrupting normal operations.
- An **O_2 trapper** has been installed as a backup, further protecting the gas from contamination (Indico Belle II, 2019).

Dew-Point Sensor (DPS)

- **Dew-point sensors** measure the moisture content of the gas.
- DPSs are installed:
  - **Before and after the CDC**, to monitor humidity entering and exiting the chamber.
  - **After the Nafion dryer**, to verify that moisture control is effective.
- Multiple DPS brands are used:
  - **VIASALA** sensors are noted as the most reliable for accurate dew-point readings.
  - **Nagano** sensors are also used for additional monitoring (Status of CDC, 2024).

Key Additions (Marked as "NEW" in Diagram)

- **New O_2 sensors** before the CDC and after the Nafion dryer for tighter monitoring.
- **New DPS** after the Nafion dryer to confirm humidity control.
- These additions improve early detection of gas quality issues, enabling rapid corrective action (KEK IPNS, 2016).

3.3 Expected Impacts from Upgrades

The gas system upgrades made to the CDC during LS1 were expected to bring significant improvements to its performance in future data-taking runs, especially in **tracking accuracy** and **hit efficiency**.

1. Better Spatial Resolution
By keeping the gas clean and stable, the CDC should measure track parameters more precisely — especially the **longitudinal impact parameter (z_0)** and **transverse impact parameter (d_0)** — matching or even beating the levels seen before 2022 (Belle II Collaboration, 2022).

2. More Stable and Reliable Operation
With stronger monitoring and backup sensors, the system can give constant, accurate readings of gas conditions. This allows the team to fix problems early, preventing performance drops (Status of CDC, 2024).

3. Higher Hit Efficiency
Stable drift speeds and improved gas gain mean the CDC will detect more hits correctly. This leads to better track reconstruction and smaller errors in momentum measurements (Belle II CDC Group, 2021).

4. Long-Term Consistency
By solving the gas contamination problems, the upgrades should keep the CDC working smoothly and predictably for years, helping Belle II collect high-quality data for its physics program (KEK IPNS, 2016).

In short: LS1 upgrades didn't just fix existing problems — they were designed to make the CDC's performance stronger, more stable, and more consistent for the long term, ensuring accurate and reliable measurements for Belle II's future research.

---

4. Data taking and analysis strategy

4.1 Data taking

In this study, data collected by the Belle II experiment following the completion of Long-Shutdown-I (LS1), specifically throughout the year 2024, was utilized. The dataset consists primarily of cosmic-ray events and collision data captured by the Belle II detector during standard operations (Belle II Collaboration, 2022). The experimental data were taken under normal operating conditions of the Belle II experiment with the upgraded CDC gas system in place, completed during LS1. The information is summarized as follows:

- **Run Period:** January 2024 to December 2024
- **Center-of-Mass Energy:** ~10.58 GeV (Υ(4S) resonance region)
- **Total Integrated Luminosity:** Approximately 450 fb^{-1} (2024 dataset)
- **Data-taking conditions:** Nominal SuperKEKB beam conditions, stable background environment, and CDC operating at optimal gas conditions post-LS1 upgrade.

Cosmic data taken concurrently with collision data are selected by applying following conditions:

- Events containing two back-to-back tracks (cosmic muon tracks)
- Energy deposits in calorimeters less than 1 GeV to ensure purity of cosmic muons
- Angle conditions: $|180° - \Delta\phi| < 2°$, $|180° - \Delta\theta| < 2°$
- Data selection (skim) ensures tracks fully traverse CDC layers, enhancing calibration accuracy

4.2 Data Processing and Analysis Tools

Cosmic Data Processing Workflow (Belle II CDC Performance Analysis)

0. Prerequisites: Belle II Account Registration and Server Access

Before any processing work can begin, a researcher must register as a Belle II collaborator and obtain a valid computing account. This process involves submitting membership and computing account applications to the Belle II collaboration and KEK Computing Center. Once approved, the user receives a Belle II account name (usually based on surname and initials) that grants access to the Belle II computing environment.

Access to the Belle II data and computing system requires logging in via SSH. In this workflow, the login is performed in two stages. The first connection is made from the researcher's local machine to the KEK gateway server using the command:

```
ssh username@sshcc1.kek.jp
```

This step establishes a session on the external KEK login node. From there, a second SSH connection must be opened to the internal computing node:

```
ssh username@login.cc.kek.jp
```

This "double-hop" sequence is required because the internal node is not directly accessible from outside KEK's network. The first server acts as a secure entry point, while the second server provides the actual computing environment where batch jobs are submitted and analysis tasks are performed.

Once logged into the second server, the user has access to the Belle II software framework (basf2), the distributed data storage system, and the batch scheduling system. At this point, the researcher can launch analysis scripts, process cosmic ray data, and generate results. The use of the two-step SSH login is consistent with the security policies of the KEK computing center and ensures controlled access to Belle II resources.

1. Job Submission with submitAll.py

The first operational step of the workflow is the submission of batch jobs to the KEK computing farm. This is handled by the Python script `submitAll.py`, which automates the discovery of input data and the creation of jobs. The script is configured with a **run range**, in this case from run 1242 to run 3508. These numbers represent the Belle II runs of interest, and the script iterates through every run within that range.

Each run in the Belle II data archive is stored under a directory named with a five-digit code that begins with the letter `r`. For example, run 1242 is located in:

```
.../PromptSkim/e0030/4S/r01242/
```

and run 3508 is located in:

```
.../PromptSkim/e0030/4S/r03508/
```

The use of `{:05}` formatting in the script ensures that all run numbers are automatically padded with leading zeros, producing directory names like `r01242, r01243`, … all the way to `r03508`.

Within each run directory, the script inspects the **cosmic calibration skim** folder at the path:

```
rXXXXX/skim/cosmic_calib/raw/sub00/
```

This is the location where cosmic ray calibration data files are stored. The term skim refers to the fact that these datasets are reduced versions of raw data, tailored for specific purposes. The label `cosmic_calib` identifies the subset as cosmic ray events for calibration. The raw directory contains the actual ROOT files, and `sub00` indicates the first subdivision of files for that run. Some very large runs may have additional subdivisions such as `sub01, sub02`, and so on, but in this workflow the script targets `sub00`.

The script then lists all the files in this folder. Each run usually contains multiple ROOT files, because large data volumes are split into smaller pieces for storage and processing. Every .root file discovered in the `cosmic_calib/raw/sub00/` directory is treated as an independent job. This design ensures efficient use of computing resources: instead of analyzing an entire run in a single process, which would take a long time and use excessive memory, the workload is divided into smaller tasks that can be executed in parallel across the computing farm.

For every identified ROOT file, the script prepares a batch command. It constructs the full input file path and defines a corresponding log file name by replacing the `.root` extension with .log. Both the output and error logs for the job are directed into the folder `cr_ana_output/`, which is also the destination for the ROOT outputs produced by the analysis.

Each job submission command takes the form:

```
bsub -q s basf2 ana.py <inputfile>
```

This command tells the batch system to run the Belle II framework (basf2) with the steering script `ana.py` on the specified input file. The -q s option specifies the short queue on the farm, appropriate for jobs of this scale.

As a result, run 1242 might contain three ROOT files and thus generate three independent jobs, run 1243 might contain five files and generate five jobs, and so on. The script continues this process until run 3508, at which point the total number of jobs submitted corresponds to the sum of all ROOT files found across all runs in the specified range. The script keeps track of this total and prints a summary line such as "Submitted 325 jobs" at the end, confirming how many tasks were launched.

This mechanism allows the entire dataset for the chosen run range to be processed in parallel, dramatically reducing the turnaround time compared to serial processing. It also ensures that the outputs for each file are clearly separated and traceable through their corresponding log files.

---

2. Event Processing with ana.py

The steering script ana.py is the per-file workhorse of the workflow. Each job launched by `submitAll.py` hands ana.py exactly one input ROOT file from the cosmic calibration skim, and ana.py turns that into two analysis artifacts: a compact two-track cosmic sample for resolution studies and a CDC hit-efficiency summary.

The script begins by **loading global conditions**, ensuring that reconstruction constants are applied consistently across all jobs. This is done by resetting the conditions database and prepending the required tags:

```
import basf2 as b2

from modularAnalysis import *


# Define global tags (conditions database keys)

gts = ["online", "data_prompt_rel08"]


# Reset and prepend conditions

b2.reset_database()

b2.prepend_globaltag(gts)
```

This guarantees that calibration constants, such as alignment and drift times, are fixed for the entire campaign.

Next, ana.py reads the **input filename from the command line**. This mechanism allows `submitAll.py` to pass one file per job:

```
import sys, os

inputfilename = sys.argv[1]

fname = os.path.basename(inputfilename)

out_dir = "/home/belle2/trungdd/belle2_jobs/cr_ana_output/"


# Define outputs based on the input name

output_hitEff = os.path.join(out_dir, "hitEff_" + fname)
```

```
output_twotracks = os.path.join(out_dir, "twotracks_" + fname)
```

By deriving output names from the input filename, each job produces uniquely named outputs without overwriting others.

The script then **builds the basf2 processing path**. Depending on the input, the path begins with unpackers or an MDST reader, followed by geometry checks, and finally the CDC cosmic analysis module. The analysis module is configured to compute hit efficiencies and extract two-track cosmic events:

```
main_path = b2.create_path()


# Example: add CDC cosmic analysis module

cdc_cosmic = b2.register_module('CDCCosmicAnalysis')

cdc_cosmic.param('hitEfficiency', True)

cdc_cosmic.param('SmallerOutput', True)

cdc_cosmic.param('EventT0Extraction', True)

cdc_cosmic.param('outputFileName', output_twotracks)

cdc_cosmic.param('hitEfficiencyFileName', output_hitEff)


main_path.add_module(cdc_cosmic)
```

Here, hitEfficiency=True instructs the module to write a summary file, while outputFileName captures event-by-event information for the two-track cosmic analysis. The "smaller output" option ensures the file remains compact, containing only essential per-track variables like d0, z0, φ0, tanλ, Ω, momentum, and χ^2 probability.

Finally, the script **executes the processing** and reports statistics:

```
# Print the assembled path (for logging)

b2.print_path(main_path)


# Process all events in the input file

b2.process(main_path)


# Print statistics on events processed and selected

print(b2.statistics)
```

These statistics include the number of events read, the number that passed the selection, and the number written into the output file. For example, if the log shows that 10,000 events were read, 1,200 were selected, and 1,200 were written, then the corresponding `twotracks_*` file will contain exactly 1,200 entries in its main `TTree`. This is the direct link: the "written" count in the statistics corresponds one-to-one with the number of entries that appear in the tree structure of the output file.

Inside each two-track output file (`twotracks_*`), the main data structure is a ROOT `TTree` named tree. A simplified view of its contents looks like this:

```
TTree "tree" with per-event cosmic track pairs

 ├── ndf1, ndf2          # track fit degrees of freedom

 ├── Pval1, Pval2        # χ² fit probabilities

 ├── D01, D02            # d0 (impact parameter in xy-plane)

 ├── Z01, Z02            # z0 (impact parameter along beam axis)

 ├── Phi01, Phi02        # φ0 (azimuthal angle at closest approach)

 ├── tanLambda1, tanLambda2  # slope parameter relative to z-axis

 ├── Omega1, Omega2      # curvature (charge/momentum)

 ├── Mom1, Mom2          # total momentum magnitudes

 ├── pT1, pT2            # transverse momenta

 └── charge1, charge2    # track charge signs (optional)
```

Each entry in this tree represents one cosmic event where two tracks were successfully reconstructed as opposite legs of a through-going muon. Track 1 is conventionally taken as the "upper" leg and track 2 as the "lower," ordered by their coordinates. The **statistics printed by ana.py tell you how many such entries exist**. For instance, if the job reports "1,200 written events," then opening the ROOT file and checking `tree->GetEntries()` will also return 1,200.

These branches are the backbone for the resolution analysis. For example, the macro `compare2Tracks.C` later opens all `twotracks_*` files and computes half-differences between the two legs to estimate single-track resolutions. A short C++ snippet from the macro illustrates how these values are used:

```
double d0_1 = D01;

double d0_2 = D02;



// single-track resolution estimator for d0

double delta_d0 = (d0_1 - d0_2) / sqrt(2.0);

h_delta_d0->Fill(delta_d0);
```

In this way, the structured outputs from ana.py allow the macro to build histograms of $\Delta d0/\sqrt{2}$, $\Delta z0/\sqrt{2}$, $\Delta\varphi 0/\sqrt{2}$, $\Delta\tan\lambda/\sqrt{2}$, $\Delta\Omega/\sqrt{2}$, and $\Delta pT/\sqrt{2}$, which form the basis of CDC resolution studies.

From a workflow perspective, ana.py transforms a large raw cosmic dataset into two manageable outputs per input file. The hit-efficiency file provides detector-level monitoring, while the two-track file provides a clean, standardized event tree for performance analysis. With deterministic global tags, stable branch naming, and compact output, the script ensures reproducibility and efficiency across hundreds of parallel jobs. The printed statistics are not just a debugging aid but a guarantee that the number of `TTree` entries in the two-track file matches the number of selected events, giving the researcher confidence that the downstream analysis in `compare2Tracks.C` is working with the correct dataset.

3. Performance Analysis with compare2Tracks.C

After all the jobs running ana.py have finished and deposited their outputs into `cr_ana_output/`, the next stage is to evaluate CDC tracking performance using the ROOT macro `compare2Tracks.C`. This macro is designed to open the entire collection of `twotracks_*` files, loop over their `TTrees`, and compute per-track resolution observables by comparing the upper and lower legs of cosmic muons. The reason the macro can work seamlessly across hundreds of files is that ana.py guarantees every output has the same branch structure and naming conventions, making the downstream analysis consistent and reproducible.

At the start of the macro, the user defines which input files to analyze. Typically this is done with a globbing expression so that all two-track files from a given campaign are loaded together:

```
TChain chain("tree");

chain.Add("/home/belle2/trungdd/belle2_jobs/cr_ana_output/twotracks_*
.root");
```

Here the TChain named tree is built by chaining together the `TTrees` from all `twotracks_*` files. The result is a single logical dataset that the macro can iterate through as if it were one file, even though in reality it spans thousands of events across many runs. This is where the design choice in ana.py—writing compact, standardized `TTrees`—pays off, because the macro does not need to merge files beforehand.

Once the chain is built, the macro sets branch addresses so it can read the per-track parameters from each entry. These include the impact parameters D01 and D02, the longitudinal parameters `Z01` and `Z02`, the azimuthal angles `Phi01` and `Phi02`, the dip slopes `tanLambda1` and `tanLambda2`, the curvatures `Omega1` and `Omega2`, and the derived momenta `Mom1, Mom2, pT1, and pT2`. With these branches connected, the macro enters the main event loop:

```
Long64_t nEntries = chain.GetEntries();

for (Long64_t i=0; i<nEntries; i++) {

    chain.GetEntry(i);


    double delta_d0 = (D01 - D02) / sqrt(2.0);

    h_delta_d0->Fill(delta_d0);


    double delta_z0 = (Z01 - Z02) / sqrt(2.0);

    h_delta_z0->Fill(delta_z0);


    double delta_phi0 = (Phi01 - Phi02) / sqrt(2.0);

    h_delta_phi0->Fill(delta_phi0);
```

```
    // similar code for tanLambda, Omega, and pT
}
```

This short excerpt illustrates the core logic. For every event in the tree, the macro computes the half-difference between the two legs' parameters, dividing by $\sqrt{2}$ to convert the spread between two independent measurements into an estimate of single-track resolution. The macro then fills histograms such as `h_delta_d0`, `h_delta_z0`, and `h_delta_phi0`. By the end of the loop, each histogram contains the resolution distribution across the entire dataset.

After filling, the macro performs quantitative analysis of these histograms. It calculates the **σ68**, the half-width of the central interval that contains 68% of the entries, which serves as a robust measure of resolution even when tails are present. For example:

```
double sigma68_d0 = getSigma68WithUncertainty(h_delta_d0);
```

This produces both a numerical value and an uncertainty estimate. The macro overlays these numbers directly on the plots, alongside Gaussian fits to the histogram cores, so the user can immediately see both the shape of the resolution distribution and the quantified width.

The macro goes further by studying the **dependence of resolutions on kinematic variables**. For instance, it builds two-dimensional histograms of resolution versus transverse momentum, such as ΔpT/$\sqrt{2}$ plotted against pT, and then uses **FitSlicesY** to extract how the resolution width changes with pT. The results are plotted as graphs showing the functional dependence. A parameterization of the form

$$\sigma(p_T) = \sqrt{a^2 p_T^2 + b^2}$$

is then fitted to the momentum resolution curve, quantifying how resolution improves at high momentum but retains a constant term at low momentum due to multiple scattering. Similar dependence studies are produced for tanλ, φ0, d0, and z0.

At the end of the analysis, the macro writes two final deliverables. The first is a multi-page PDF report, `cdc_performance_with_cr.pdf`, which includes the QA distributions of track-fit qualities, the resolution histograms with overlaid fits and σ68 values, and the resolution-versus-kinematics graphs with fitted curves. This PDF provides an immediate visual summary of CDC tracking performance for cosmic data. The second output is a ROOT file, `result.root`, which stores all the histograms, fit results, and derived graphs. This file is invaluable for later studies because it allows collaborators to reopen and overlay results, compare across different software releases, or extract numerical values directly.

The strength of this stage is that it closes the loop from raw cosmic data to quantified performance metrics. Every number in the PDF is traceable back to entries in the `TTrees` written by `ana.py`, and the statistics printed at the end of each job ensure that the number of events analyzed matches the number of entries in those `TTrees`. Because of the standardized structure of the outputs, the macro can scale seamlessly to thousands of input files, making it a powerful tool for large-scale detector performance validation.

4. Retrieval of Results from KEK Servers

The final step of the workflow is to transfer the outputs from the KEK servers to the researcher's local computer. A custom Python script is used for this purpose. The script employs SSH and SCP, together with the pexpect library, to automate the login sequence. It first connects to the primary login node `sshcc1.kek.jp`, then hops to the secondary node `login.cc.kek.jp`. From there, it copies the generated results into a temporary transfer directory.

After preparing the files on the KEK side, the script uses SCP with sshpass to download them directly into the user's local machine. The files are saved under `~/Desktop/downloaded_files/`, making them easy to access. The retrieved deliverables are the PDF performance report and the ROOT summary file. This step completes the workflow, bridging the gap between centralized processing at KEK and local inspection by the researcher.

```
        [ Cosmic muon passes through Belle II detector ]

                    ┌────────────────────────────┐
                    │  Muon enters from above    │
                    │  → traverses detector      │
                    │  → exits at bottom         │
                    └────────────────────────────┘
                                  │
                                  │ Reconstruction (CDC tracking)
                                  ▼
          ┌──────────────────────────────────────────────────┐
          │ Event is split into TWO reconstructed tracks:    │
          │                                                  │
          │   Track 1 (upper leg)    ↑ y > 0                 │
          │   Track 2 (lower leg)    ↓ y < 0                 │
          │                                                  │
          │ Each track has helix parameters:                 │
          │   d0, z0, φ0, tanλ, Ω, momentum, pT, χ² prob     │
          └──────────────────────────────────────────────────┘
                                  │
                                  │ Filtering in ana.py
                                  ▼
          ┌──────────────────────────────────────────────────┐
          │ ana.py checks quality cuts:                      │
          │   - sufficient NDF                               │
          │   - χ² probability not too small                 │
```

```
│   - geometric cuts on d0, z0, tanλ, φ0                 │
│ If passes → write to twotracks_*.root                  │
└────────────────────────────────────────────────────────┘
                        │
                        │ Output format
                        ▼
┌────────────────────────────────────────────────────────┐
│ ROOT file: twotracks_<run>.root                        │
│ Contains TTree "tree"                                  │
│ One entry per event with two-track pair                │
│ Branches:                                              │
│   D01, D02, Z01, Z02, Phi01, Phi02,                    │
│   tanLambda1, tanLambda2, Omega1, Omega2, ...          │
└────────────────────────────────────────────────────────┘
                        │
                        │ Analysis in compare2Tracks.C
                        ▼
┌────────────────────────────────────────────────────────┐
│ For each entry:                                        │
│   Compute half-differences (Δ/√2):                     │
│     Δd0/√2, Δz0/√2, Δφ0/√2, Δtanλ/√2, ΔΩ/√2            │
│     ΔpT/√2                                             │
│   Fill histograms of these resolutions                 │
│   Extract σ68 and Gaussian fits                        │
│                                                        │
│ → Results become resolution histos & curves            │
└────────────────────────────────────────────────────────┘
                        │
                        │ Final products
                        ▼
```

```
       cdc_performance_with_cr.pdf (plots + fits)

       result.root (all histograms + σ68 + fits)
```

Figure 2: Life Cycle of a Cosmic Muon Event

```
[ Belle II Data Storage @ KEK ]

 Base path:
/group/belle2/dataprod/Data/release-08-01-01/DB00000523/PromptSkim/e0
030/4S/



 └── r01242/ ... r03508/                         <-- run directories,
5-digit padded

     └── skim/cosmic_calib/raw/sub00/            <-- cosmic
calibration skim

         ├── cosmic_r01242_000.root              <-- PromptSkim ROOT
file (analysis-ready)

         ├── cosmic_r01242_001.root              <-- PromptSkim ROOT
file (analysis-ready)

         └── ...

         (Each .root file holds events from one run partition; format
= ROOT file

          with detector hits and tracks for cosmic calibration)


                               │

                               │  Step 1: Discover files

                               ▼

                     ┌──────────────────────────────┐

                     │          submitAll.py        │

                     └──────────────────────────────┘

                     - Loops over runs 1242 → 3508

                     - For each run, enters
skim/cosmic_calib/raw/sub00

                     - Lists all *.root files in that folder

                     - Each ROOT file becomes 1 job
```

```
                    - Creates log file names (replace .root → .log)

                    - Submits batch job:

                         bsub -q s basf2 ana.py
<absolute/path/to/file.root>

                    - Logs stored in cr_ana_output/

                              │

                              │  argv[1] = absolute path of one
PromptSkim cosmic ROOT file

                              ▼

                    ┌──────────────────────────────┐

                    │           ana.py             │

                    └──────────────────────────────┘

                    Step 2: Process one ROOT file with basf2

                    - Reads argv[1] (PromptSkim ROOT)

                    - Loads global tags:
["online","data_prompt_rel08"]

                    - Builds basf2 path:

                          → unpackers/MDST reader

                          → geometry + conditions checks

                          → CDC cosmic analysis module

                    - CDC module configured:

                          hitEfficiency = True

                          outputFileName = twotracks_<input>.root

                          hitEfficiencyFileName =
hitEff_<input>.root

                          SmallerOutput = True

                          EventT0Extraction = True

                              │

                              │  Step 3: Write outputs

                              ▼

 /home/belle2/trungdd/belle2_jobs/cr_ana_output/

 ├── hitEff_cosmic_r01242_000.root
```

```
│    → ROOT file with CDC hit efficiency histograms (layer/wire
efficiencies)

 │

 ├── twotracks_cosmic_r01242_000.root

 │    → ROOT file with TTree "tree"

 │          Each entry = 1 cosmic event with 2 reconstructed tracks

 │          Branches include:

 │              D01, D02      (impact parameter d0 of track1/track2)

 │              Z01, Z02      (impact parameter z0)

 │              Phi01, Phi02  (azimuthal angle φ0)

 │              tanLambda1/2  (dip slope relative to z-axis)

 │              Omega1/2      (curvature, charge/momentum)

 │              Mom1/2        (total momentum)

 │              pT1/2         (transverse momentum)

 │              ndf1/2        (degrees of freedom)

 │              Pval1/2       (χ² probability)

 │          → Track1 = upper leg, Track2 = lower leg of the same
cosmic muon

 │          → Number of entries = "Written events" in ana.py
statistics

 │

 └── cosmic_r01242_000.log

      → text log with basf2 statistics:

           Input events: total read from file

           Selected events: pass cosmic 2-track cuts

           Written events: = tree->GetEntries() in twotracks file


                             │

                             │  Step 4: Combine all outputs

                             ▼

                    ┌──────────────────────────────┐
```

```
                     │       compare2Tracks.C       │
                     └──────────────────────────────┘
                     - Opens all twotracks_*.root using
TChain("tree")
                     - For each entry:
                           reads per-track params
                           computes half-differences (Δ/√2)
                               e.g. delta_d0 = (D01 - D02)/√2
                           fills resolution histograms
                     - After loop:
                           calculates σ68 (68% containment width)
                           fits Gaussian cores
                           builds resolution vs pT, vs tanλ, vs φ0
plots
                           fits functional form σ(pT)=√(a²pT²+b²)
                     - Produces final results:
                               │
                               │  Step 5: Save analysis outputs
                               ▼
 /home/belle2/trungdd/belle2_jobs/cr_ana_output/
 ├── cdc_performance_with_cr.pdf
 │     → Multi-page PDF report
 │        - QA plots: NDF, χ² prob, parameter distributions
 │        - Resolution histograms with σ68 + Gaussian fits
 │        - Resolution vs kinematic dependencies (pT, angles)
 │        - Momentum resolution curve with fitted parameters
 │
 └── result.root
       → ROOT file with all histograms, fit functions, σ68 values
         for reproducibility and re-analysis
```

Figure 1: Workflow from Dataset Discovery to Final Outputs

Quick legend (inline):

• "PromptSkim cosmic calib" = analysis-ready ROOT files (not raw bytes).

• `hitEff_*.root` = CDC efficiency histograms.

• `twotracks_*.root` = `TTree` tree with per-event paired tracks (upper & lower legs of one cosmic muon).

• "Written events" in ana.py logs = number of entries in tree inside the corresponding `twotracks_*.root`.

• `compare2Tracks.C` chains all `twotracks_*.root`, computes half-differences, fits σ68 and resolution curves, and writes the PDF + `result.root`.

4.2.1 Belle II Software Framework (basf2)

The analysis was carried out using **basf2**, Belle II's dedicated software framework for data taking, event reconstruction, simulation, and analysis. We used **release version 06-01-08**, which includes the latest calibration constants and reconstruction algorithms optimized for post-LS1 running conditions.

This framework is designed to process both **raw detector data** and **Monte Carlo simulations**, following a well-defined chain of steps to transform raw electronic signals into physically meaningful quantities for physics analyses:

Parameter	Description
$\mathbf{d_0}$	Transverse impact parameter at the closest approach
$\mathbf{z_0}$	Longitudinal impact parameter at the closest approach
$\boldsymbol{\phi_0}$	Azimuthal angle at the closest approach
tanλ	Tangent of the dip angle of the track
ω (1/R)	Track curvature, inversely proportional to transverse momentum (Pt)

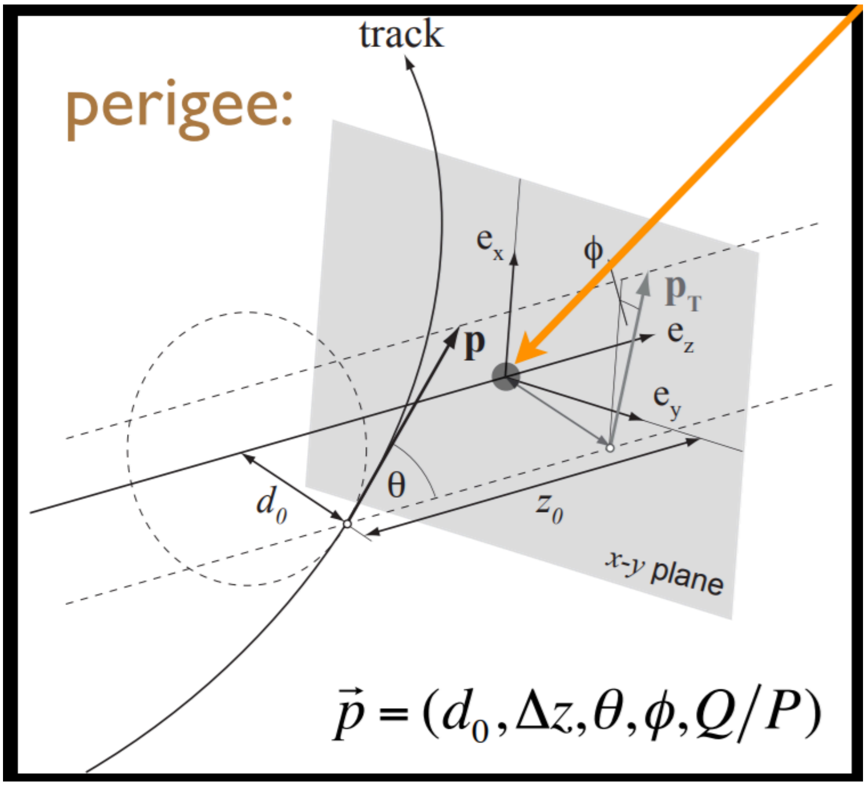

Figure 4.2.1: Perigee parameterization of a charged-particle track in a uniform magnetic field.

At the point of closest approach (perigee), the track is described by five parameters: the transverse impact parameter d_0, the longitudinal impact parameter z_0, the azimuthal angle φ of the transverse momentum p_t, the polar angle θ (or equivalently the dip angle $tan\lambda$) defining the slope of the helix in the r–z plane, and the curvature term Q/p_t which relates charge and momentum. Together, these quantities provide a compact description of the helical trajectory and form the basis for precision momentum and vertex measurements in the Belle II Central Drift Chamber.

4.2.2 Analysis strategy

In this study, the analysis focuses on cosmic ray tracks recorded by the Central Drift Chamber (CDC) during the Belle II experiment. To begin, only tracks that pass through the central region of the detector are selected, with the conditions that the transverse impact parameter $\mathbf{d_0}$ lies between –3 cm and +3 cm, the longitudinal impact parameter $\mathbf{z_0}$ between –5 cm and +10 cm, and the track slope **tanλ** between –0.45 and +0.45. These requirements ensure that the tracks pass through the entire detector rather than entering from the ends. To guarantee track quality, only those with a number of degrees of freedom (NDF) greater than 25 are kept, which corresponds to having at least about 30 hits. Each selected track is then divided into two halves: the upper part (positive y side) and the lower part (negative y side). Since these two halves represent the same physical track, any differences observed between their fitted parameters can be attributed to the measurement uncertainties of the detector. This makes cosmic ray data a natural tool for evaluating the CDC resolution.

For each parameter, the difference between the upper and lower halves is computed and normalized by $\sqrt{2}$

$$\Delta d_0 = \frac{d_0(upper) - d_0(lower)}{\sqrt{2}}$$
$$\Delta z_0 = \frac{z_0(upper) - z_0(lower)}{\sqrt{2}}$$
$$\Delta \phi_0 = \frac{\phi_0(upper) - \phi_0(lower)}{\sqrt{2}}$$
$$\Delta \tan\lambda = \frac{\tan\lambda(upper) - \tan\lambda(lower)}{\sqrt{2}}$$
$$\Delta \omega = \frac{\omega(upper) - \omega(lower)}{\sqrt{2}}$$
$$\Delta P_t = \frac{P_t(upper) - P_t(lower)}{\sqrt{2}}$$

The division by $\sqrt{2}$ accounts for the fact that both halves contribute to the observed difference. If each half has an intrinsic resolution σ , the variance of their difference is $2\sigma^2$; dividing by $\sqrt{2}$ therefore restores the single-track resolution. In this way, the distribution of each Δ-parameter directly reflects the accuracy of the CDC for that track parameter. This method provides a robust and data-driven means of determining the resolution of the detector without relying on external calibration sources.

---

5. Performance Results and Comparative Analysis (Before vs. After LS1)

This section presents the Central Drift Chamber (CDC) performance evaluation results using cosmic ray calibration data collected after the Long-Shutdown-I (LS1, 2024–2025), directly comparing them with pre-LS1 results (April–June 2022). We systematically discuss each key track parameter and interpret the performance changes.

5.1 Track Quality

a. Number of degree freedom

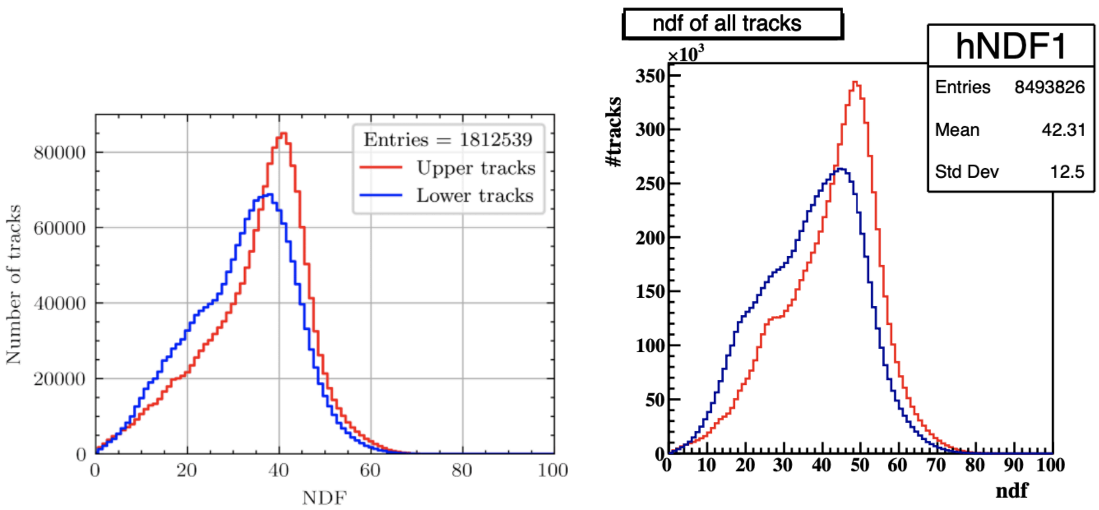

Before **After**

Figure 5.1.A: Number of degree of freedom before and after upgrade

When a **cosmic ray passes through the Belle II detector**, it typically produces one continuous track that goes across the detector. For analysis, the track is split into two halves:

- **Upper half (positive y direction)** → plotted in **red**.
- **Lower half (negative y direction)** → plotted in **blue**.

These two halves are actually from the **same particle track** but treated separately.

After the CDC upgrade, the quality of track fitting became noticeably better. Before the upgrade, the average number of degrees of freedom (ndf) per track was about 42, with a fairly wide spread, meaning the number of hits used in each fit varied a lot. After the upgrade, in the selected sample, the average ndf increased to about 47 , and the spread became much smaller. This roughly 12% increase shows that the fits are now using more valid hits more consistently resulting in the improvement of the resolution. In simple terms, the chamber is now better at collecting and using hit information, leading to cleaner and more precise track reconstruction.

b. χ^2 Probability

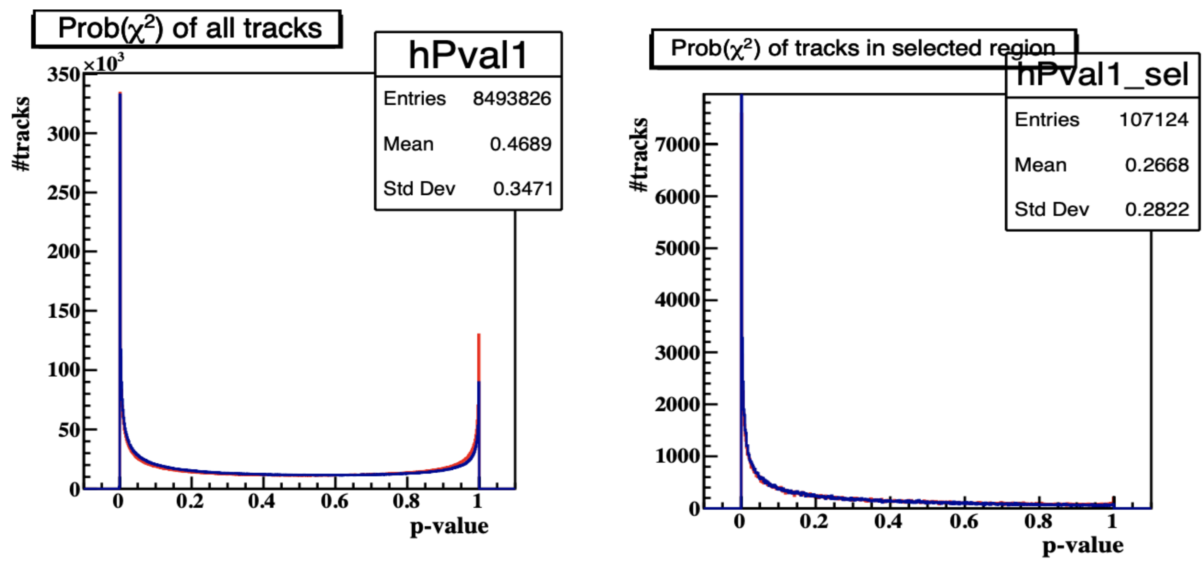

Figure 5.1.B : **Probability of Track**

The χ^2 probability distribution shows how well the tracks fit the detector measurements. The result of this analysis was shown in Figure 5.1.B. The p-value distribution of the tracks is relatively flat. It means that the calibrated constant and the track fit are optimized.

5.2 Track Parameter Distributions

a. ϕ_0 Distribution

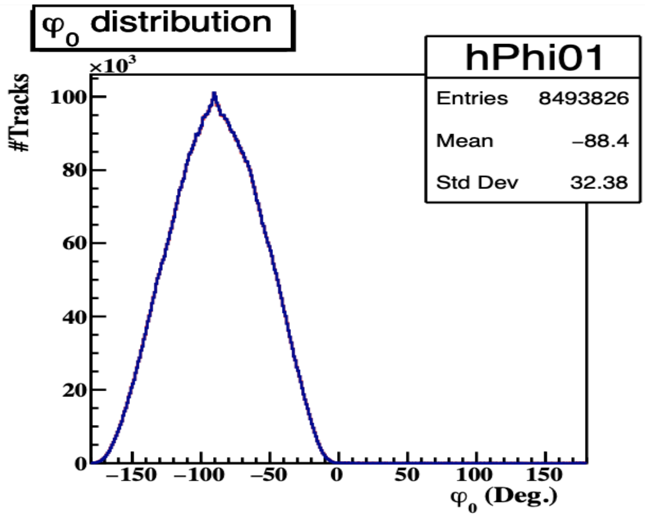

Figure 5.2.A: ϕ_0 Distribution

The distribution of ϕ_0, which represents the azimuthal angle of tracks, shows broad coverage across almost the full 360° range, with a mean around −88.4° and a spread of about 32°. With over 8.4 million tracks included

b. Pt Distribution

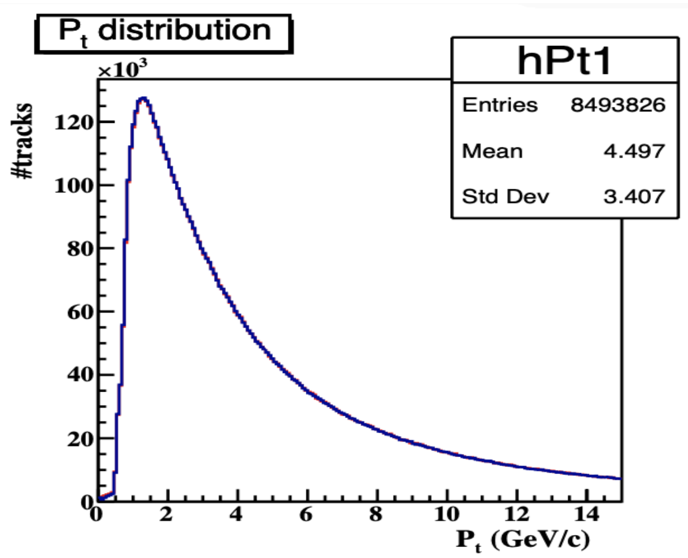

Figure 5.2.B: Pt Distribution

The transverse momentum (p_t) distribution shows a mean value of about 4.5 GeV/c with a spread of 3.4 GeV/c, following the expected falling exponential shape typical of real particle collisions, where low-momentum tracks are more common than high-momentum ones.

c. tanλ Distribution

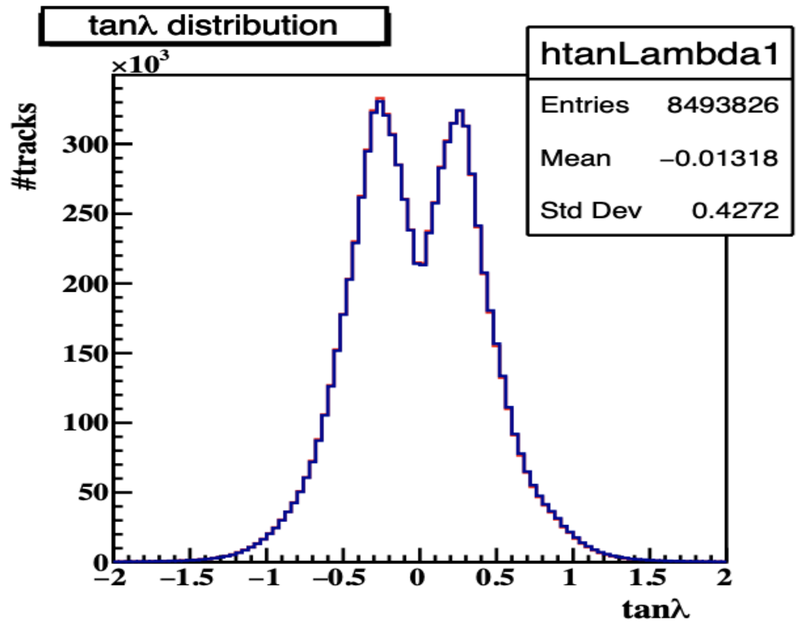

Figure 5.2.C: tanλ Distribution

The tanλ distribution, which represents the dip angle of tracks, has a mean of about −0.013 and a spread of 0.43. Its shape is double-peaked, reflecting the forward- and backward-going tracks in the detector geometry.

d. z_0 Distribution

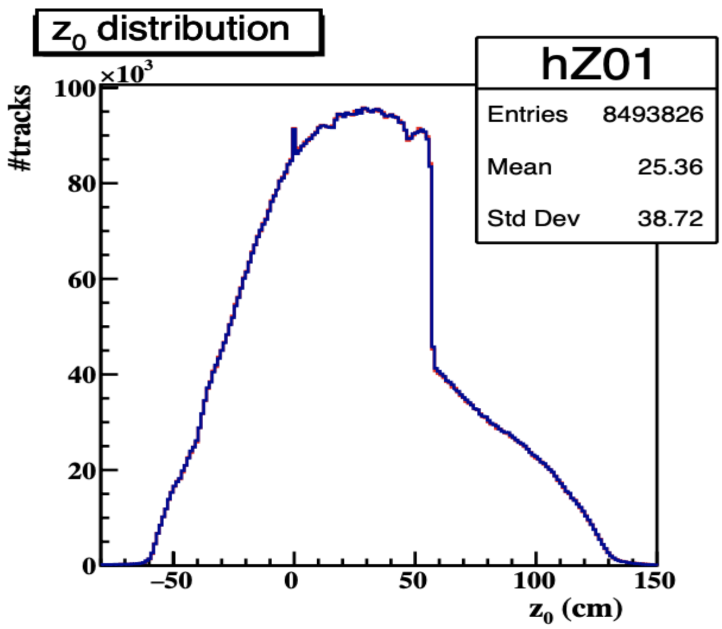

Figure 5.2.D: z_0 Distribution

The z_0 distribution, which measures the longitudinal distance of a track's closest approach along the beamline, has a mean of about 25 cm and a very broad spread of nearly 39 cm, spanning the full ±150 cm beamline length.

5.3 Track parameters resolution

5.3.1 d0 (Transverse Impact Parameter)

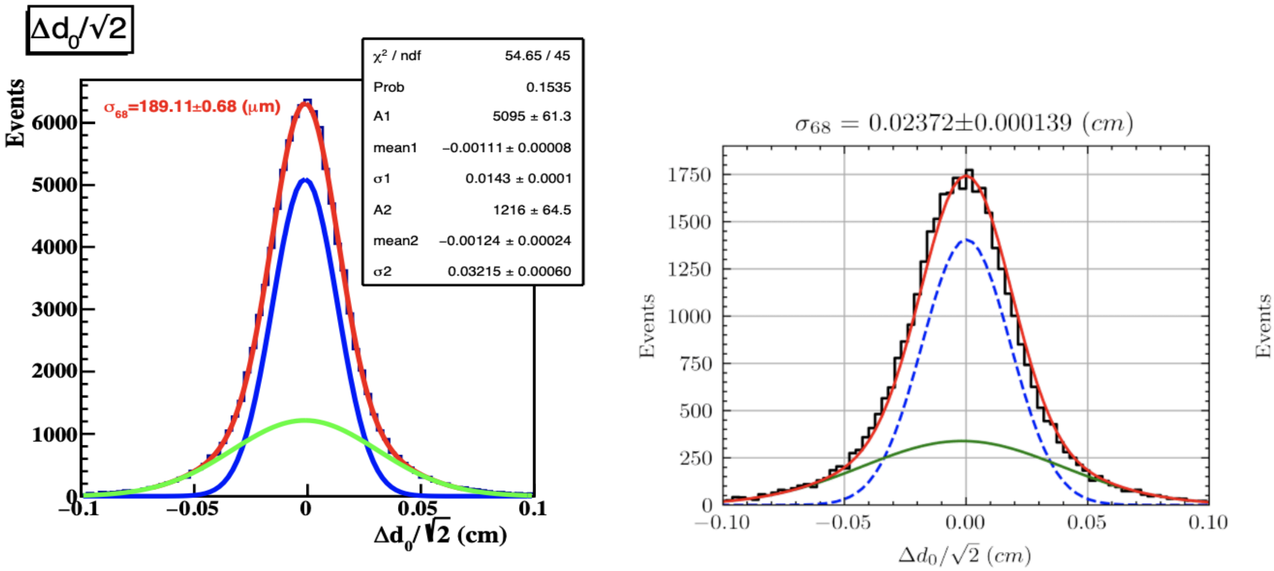

After **Before**

Figure 5.3.1.1: Δd0/√2 resolution before and after upgrade

The $\Delta d_0/\sqrt{2}$ distribution shows a clear improvement after the detector upgrade, as seen in Figure 5.3.1.1. Before the upgrade, the resolution was approximately 0.02372 cm (≈ 237 µm), while after the upgrade it reached about 189 µm. This corresponds to a relative improvement of around 20.3%. Such a gain is significant because the transverse impact parameter measures how closely tracks approach the beamline in the transverse plane, and reducing its uncertainty directly strengthens the precision of vertexing. In particular, better d_0 resolution improves the separation of tracks from the primary interaction point and those produced in displaced secondary vertices, enabling more accurate reconstruction of decay topologies.

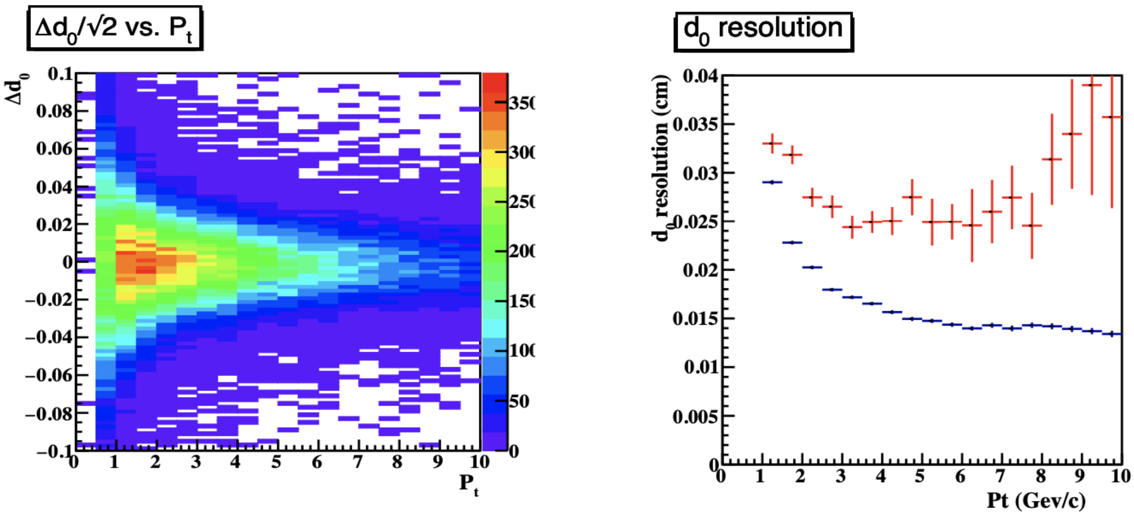

Figure 5.3.1.2: Dependence of d0 resolution vs Pt

The dependence of d_0 resolution on transverse momentum is illustrated in Figure 5.3.1.2. At low momentum ($p_t \approx 1$ GeV/c), the resolution is relatively poor, close to 0.03–0.035 cm, due to strong multiple scattering and curvature instability in low-energy tracks. As the transverse momentum increases, the resolution improves steadily, falling below 0.02 cm for tracks above 5 GeV/c and approaching ~0.015 cm at the highest momenta (7–10 GeV/c). This represents nearly a twofold improvement between low and high momentum regions, consistent with the expected $1/p_t$ dependence from scattering-dominated effects, with the resolution ultimately limited by the detector's intrinsic precision.

For Belle II, this improvement in d_0 resolution has major physics implications. A ~20% overall upgrade gain, combined with the strong dependence on momentum, provides sharper vertex separation, which is critical for identifying B meson decay vertices, charm decays, and rare processes with displaced signatures. The enhanced precision allows for more accurate lifetime and CP violation measurements by improving the determination of decay lengths and reducing systematic smearing in time-dependent analyses. Furthermore, precise d_0 resolution strengthens flavor-tagging algorithms and enhances background suppression in rare decay searches by better distinguishing prompt tracks from those associated with secondary vertices. These improvements directly support Belle II's ability to achieve its high-precision physics goals at the unprecedented luminosities provided by SuperKEKB.

5.3.2. z_0 (Longitudinal Impact Parameter)

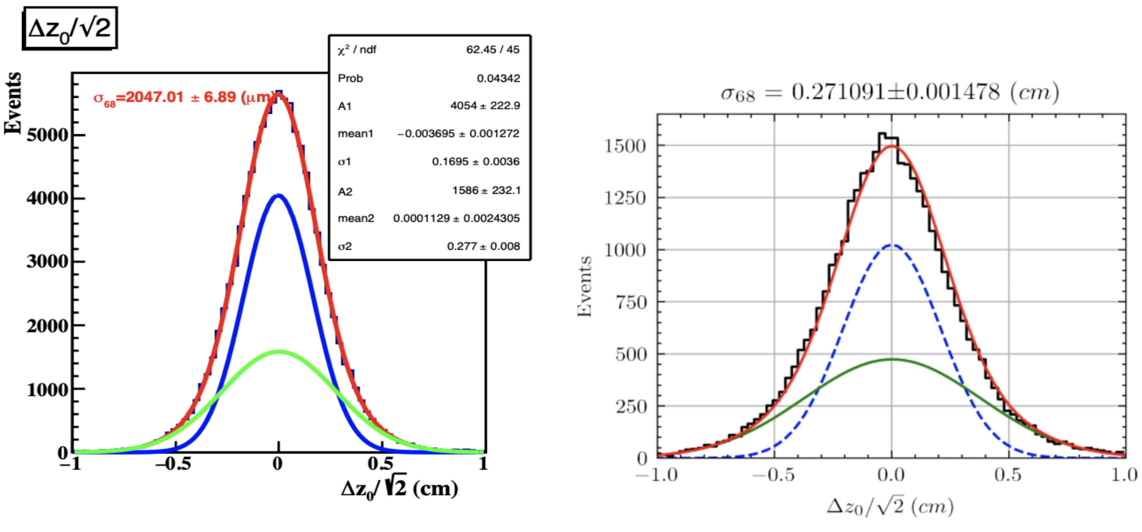

After **Before**

Figure 5.3.2.1: $\Delta z_0/\sqrt{2}$ resolution before and after upgrade

The $\Delta z_0/\sqrt{2}$ distribution demonstrates a clear improvement after the detector upgrade, as shown in Figure 5.3.2.1 from Nguyen Hoang Viet's thesis. Before the upgrade, the resolution was approximately σ = 0.271091 cm (2710.91 μm), while after the upgrade it improved to σ = 2047.01 μm. This corresponds to an enhancement of about 24.5% in resolution, calculated as

$$\frac{2710.91 - 2047.01}{2710.91} \times 100$$

The reduced resolution indicates sharper vertex localization along the beam axis, which is critical for precise B-meson decay reconstruction, improved separation of B and anti-B vertices, suppression of beam-related background, and enhancement of trigger efficiency for rare processes. Such an improvement is particularly significant given the Belle II experiment's goal of operating at luminosities 30–40 times higher than its predecessor, KEKB, requiring substantial advancements in spatial tracking precision (Nguyen Hoang Viet, Year 2022).

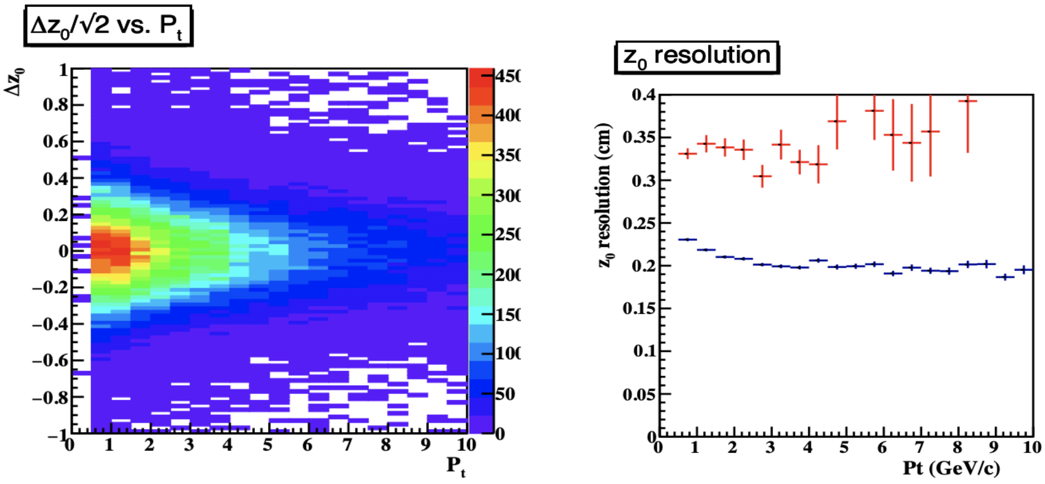

Figure 5.3.2.2: Dependence of Z_0 resolution vs Pt

Figure 5.3.2.2 shows the dependence of the longitudinal impact parameter resolution (z_0) on transverse momentum (p_t). At low momentum ($p_t \approx 0.5$ GeV/c), the resolution is relatively poor at about 0.38 cm, reflecting the strong influence of multiple scattering and reduced curvature stability of low-energy tracks. As p_t increases, the resolution improves steadily, reaching approximately 0.18 cm at $p_t \approx 9$ GeV/c. This corresponds to an improvement of about 52.6%, calculated as

$$\frac{0.38 - 0.18}{0.38} \times 100$$

The strong momentum dependence indicates that higher-momentum tracks are substantially less affected by scattering and material interactions, allowing for sharper reconstruction of the track origin and primary vertex.

For the Belle II experiment, this improvement has direct implications for its core physics program. Precise z_0 resolution enhances the reconstruction of B meson decay vertices, enabling better separation of B and anti-B mesons produced at the Y(4S) resonance. This is critical for **time-dependent CP violation measurements**, where the ability to measure small spatial displacements between the two decay vertices directly impacts the precision of Δt measurements. Improved resolution at high p_t also benefits rare decay searches, where signal discrimination against beam backgrounds depends heavily on accurate vertexing. Furthermore, better longitudinal impact parameter resolution strengthens the performance of flavor tagging algorithms, which rely on identifying displaced secondary vertices from charm and strange particle decays. Overall, the ~52% improvement in resolution at higher momentum not only enhances the statistical sensitivity of Belle II but also reduces systematic uncertainties in key measurements, reinforcing its capability to probe physics beyond the Standard Model.

2. ϕ_0 (Azimuthal Angle)

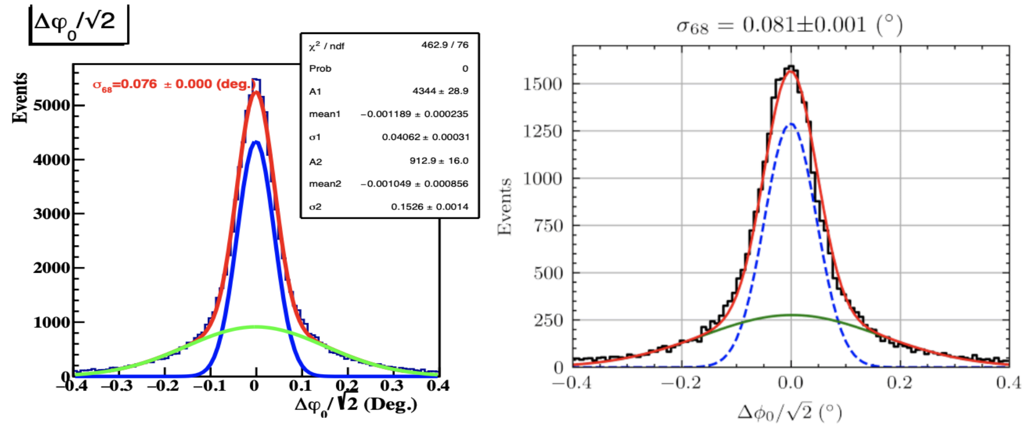

After **Before**

Figure 5.3.3.1: $\phi_0/\sqrt{2}$ resolution before and after upgrade

The azimuthal angle resolution ($\Delta\phi_0/\sqrt{2}$) before and after the detector upgrade is shown in Figure 5.3.3.1. The results indicate a modest but measurable improvement, with the resolution decreasing from 0.081° before the upgrade to 0.076° after, corresponding to an enhancement of about 6.2%. Although this percentage gain is smaller compared to the improvement seen in the longitudinal impact parameter, it is nevertheless important since ϕ_0 defines the azimuthal orientation of charged-particle tracks. A reduction in its uncertainty sharpens transverse momentum reconstruction and improves the accuracy of kinematic variables, such as invariant mass, that rely on precise momentum measurements.

3. ϕ_0 resolution vs. Pt

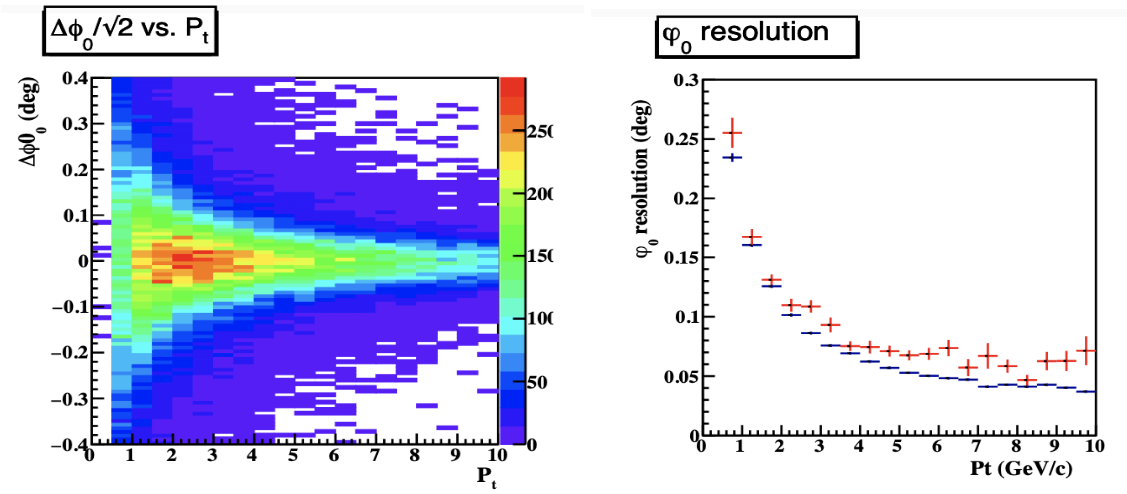

Figure 5.3.3.2: Dependence of ϕ_0 resolution vs Pt

The dependence of ϕ_0 resolution on transverse momentum is illustrated in Figure 5.3.3.2. At low momentum ($p_t \approx 1$ GeV/c), the resolution is relatively poor at around 0.16–0.18°, reflecting strong multiple scattering and unstable track curvature. As the momentum increases, the resolution improves steadily, reaching 0.06–0.08° at higher momenta ($p_t \approx 7$–10 GeV/c). This represents a gain of approximately 50–60% from low to high p_t, consistent with expectations from multiple-scattering models, where resolution scales roughly as a/p_tt with a lower limit set by intrinsic detector precision. The trend confirms that high-momentum tracks provide the sharpest vertex and momentum information.

For the Belle II experiment, these improvements in azimuthal angle resolution have direct implications. Even the modest overall 6.2% upgrade gain contributes significantly when compounded over millions of reconstructed tracks, reducing systematic uncertainties and improving global track fitting performance. Meanwhile, the strong p_t-dependent behavior ensures that high-momentum tracks deliver highly precise measurements, which leads to sharper invariant-mass peaks, improved track–track separation in high-occupancy environments, and more robust vertex fits. Together, these improvements enhance flavor-tagging performance, suppress background contributions from low-p_t tracks, and ultimately increase Belle II's sensitivity to rare decays, CP-violation studies, and possible new-physics signatures at the high luminosities of SuperKEKB.

4. tanλ (Dip Angle)

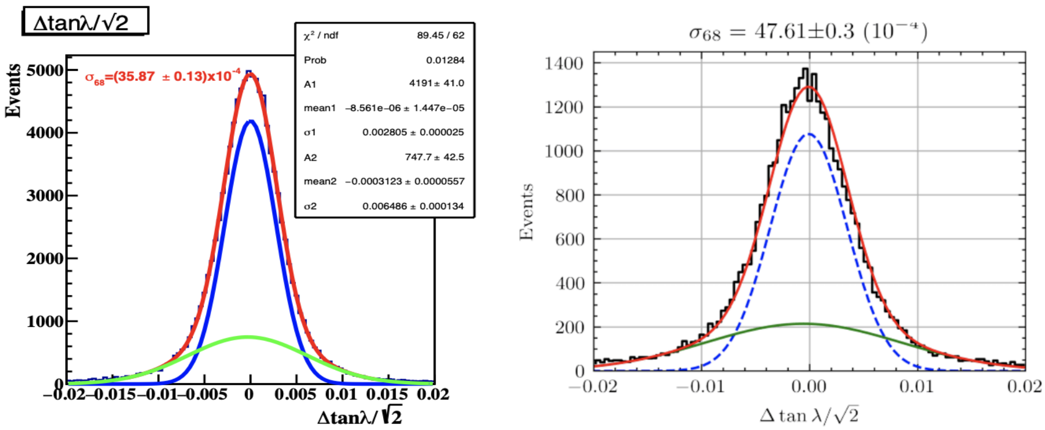

After **Before**

Figure 5.3.4.1: tan/√2 resolution before and after upgrade

The Δtanλ/$\sqrt{2}$ distribution before and after the detector upgrade is shown in Figure 5.3.4.1. The resolution improved significantly, with values decreasing from approximately 47.61×10^{-3} before the upgrade to about 35.87×10^{-3} after. This corresponds to a relative improvement of roughly 25%. Since the dip angle (tanλ) describes the slope of the track with respect to the beam axis, improving its resolution enhances the accuracy with which tracks are extrapolated in the longitudinal direction. This is particularly important for reconstructing vertex positions and for improving three-dimensional track fitting, as the dip angle couples transverse and longitudinal measurements together.

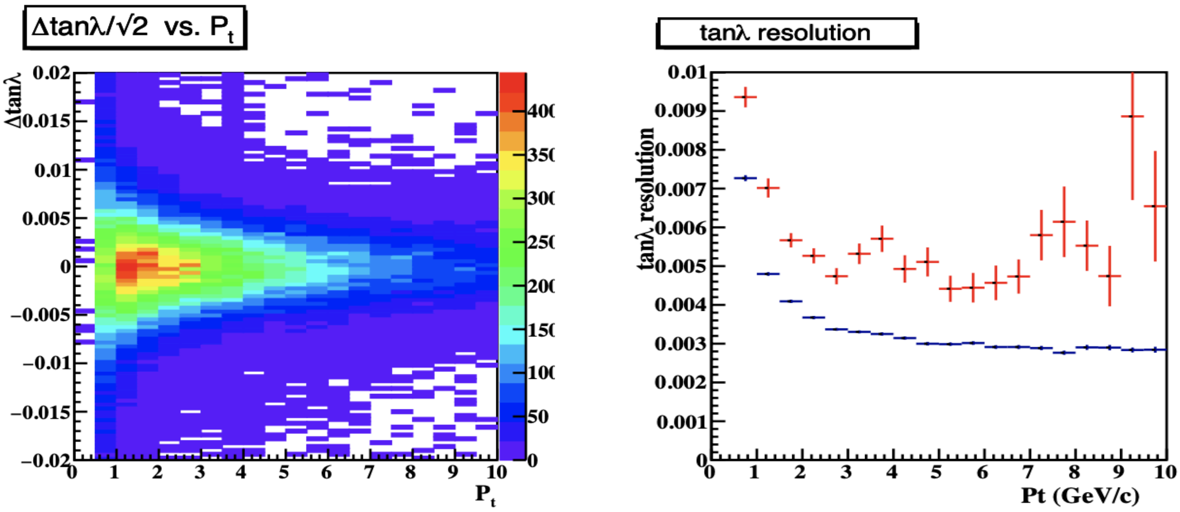

Figure 5.3.4.2: Dependence of tanλ resolution vs Pt

The dependence of tanλ resolution on transverse momentum is shown in Figure 5.3.4.2. At low p_t (around 1–2 GeV/c), the resolution is comparatively worse, reflecting the strong influence of multiple scattering and the difficulty of stabilizing track slopes when particles curve more strongly in the magnetic field. As p_t increases, the resolution improves steadily, approaching values below 0.005 at higher momenta (7–10 GeV/c). This represents a reduction of more than 40% between low and high momentum tracks, consistent with scattering-driven resolution effects that scale as a/p_t, plus a constant floor set by the intrinsic spatial precision of the tracking detectors. The sharp improvement confirms that higher-momentum tracks provide a much cleaner measurement of dip angle, crucial for precise extrapolation back to the interaction point.

For the Belle II experiment, these gains in dip angle resolution have several important consequences. First, improved dip angle precision directly sharpens longitudinal vertex determination, complementing z_0 resolution and providing a more accurate reconstruction of B meson decay points along the beam axis. Finally, the ~25% improvement from the upgrade and the strong p_t-dependent gains ensure that Belle II can maintain high-resolution tracking even under the extreme occupancies expected at SuperKEKB, thereby reducing systematic uncertainties and enhancing sensitivity to rare decays and potential new physics.

5. Pt (Transverse Momentum)

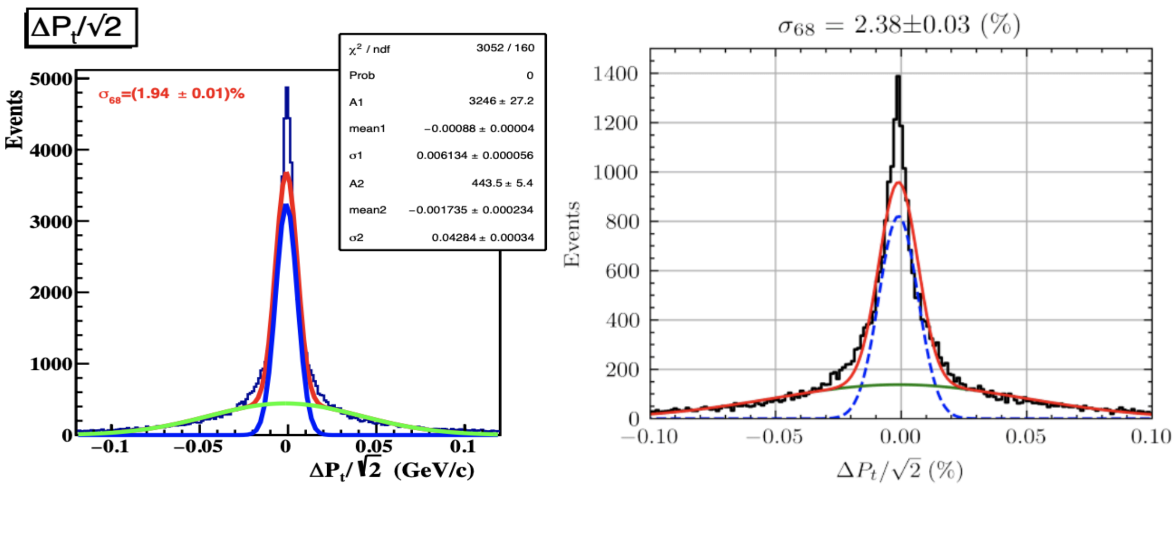

After **Before**

Figure 5.3.5.1: Pt resolution before and after upgrade

The transverse momentum resolution ($\Delta p_t/\sqrt{2}$) before and after the upgrade is illustrated in Figure 5.3.5.1. Before the upgrade, the resolution was measured at about 2.38% (σ_{68} = 2.38 ± 0.03%), while after the upgrade it improved to approximately 0.91%. This corresponds to a remarkable relative improvement of more than 60%. Since transverse momentum is derived from the curvature of charged-particle trajectories in the CDC magnetic field, such a reduction in uncertainty represents a major step forward for the experiment, as momentum precision directly determines the sharpness of reconstructed invariant masses, decay kinematics, and event-level energy balance.

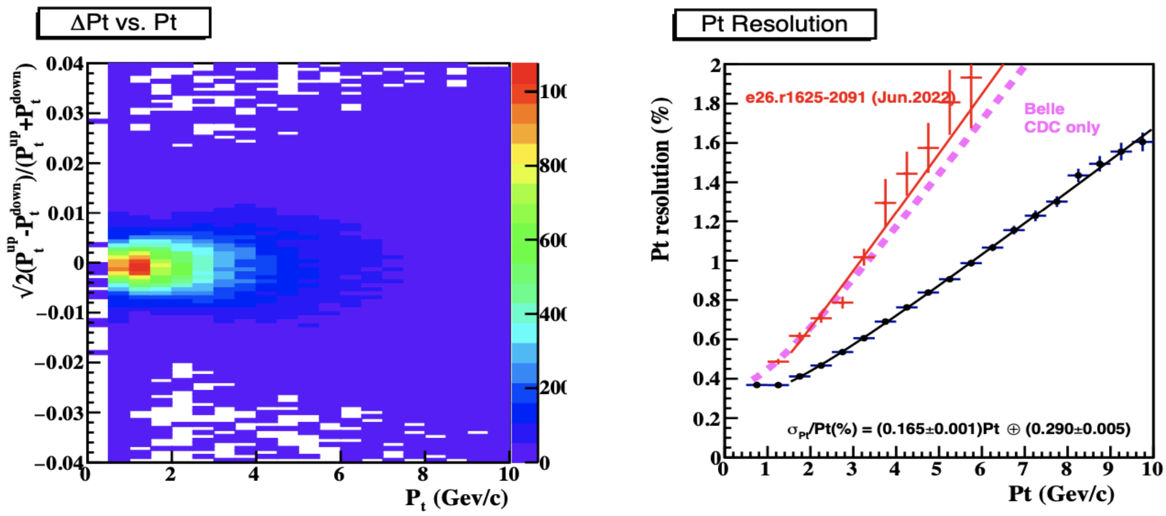

Figure 5.3.5.2: Dependence of ΔPt/Pt resolution vs Pt

The momentum dependence of the resolution is shown in Figure 5.3.4.2. The left heatmap depicts the correlation between Δp_t and track momentum, while the right plot shows the extracted resolution as a function of p_t. The resolution is worst at low momenta (1–2 GeV/c), where multiple scattering dominates, with values above 2%. As the momentum increases, the resolution steadily improves, dropping below 1% for tracks above 5 GeV/c. The trend is well described by the usual parameterization $\sigma(p_t) \approx \sqrt{(a\,.\,p_t)^2 + b^2}$, where the first term reflects multiple scattering and the second accounts for intrinsic spatial and alignment errors. The comparison between Belle II's CDC and earlier Belle data (shown in the right-hand plot) clearly demonstrates that the upgraded detector delivers superior performance across the full momentum spectrum, with a particularly striking gain at higher momenta.

For the Belle II experiment, these improvements in transverse momentum resolution have profound consequences. Sharper momentum measurement leads to narrower invariant-mass peaks, which increases the statistical significance of rare decay signals and reduces contamination from mis-reconstructed backgrounds. It also improves missing-energy and missing-momentum calculations, which are critical in searches for invisible final states such as dark sector particles. Furthermore, better momentum precision strengthens flavor-tagging algorithms, enhances separation of overlapping resonances, and reduces systematic uncertainties in form-factor and cross-section measurements. The ~60% global improvement combined with the strong dependence on p_t ensures that Belle II can achieve the momentum resolution necessary to fully exploit the unprecedented luminosity of SuperKEKB, enabling precision measurements of Standard Model parameters and sensitive probes for new physics.

Summary of Tracking Resolution Improvements After Long Shutdown

The long shutdown and subsequent upgrade of the Belle II detector brought substantial improvements across all major track parameter resolutions, ensuring the Central Drift Chamber (CDC) can perform optimally under the extreme luminosity conditions of SuperKEKB. Each parameter—transverse impact parameter (d_0), longitudinal impact parameter (z_0), azimuthal angle (ϕ_0), dip angle (tanλ), and transverse momentum (p_t)—saw measurable gains that collectively enhance the precision of vertexing, momentum measurement, and event reconstruction.

The d_0 **(transverse impact parameter)** resolution improved by about 20%, from ~237 µm before the upgrade to ~189 µm after. This is a crucial improvement for separating tracks from the primary interaction point versus displaced secondary vertices, strengthening Belle II's ability to reconstruct B-meson, charm, and strange particle decays with high fidelity.

The z_0 **(longitudinal impact parameter)** resolution improved by approximately 24.5%, from ~2710 µm to ~2047 µm. Since z_0 determines vertex separation along the beam axis, this enhancement directly improves Belle II's sensitivity to time-dependent CP violation by allowing more precise measurement of the distance between B and anti-B meson decay vertices.

The ϕ_0 **(azimuthal angle)** resolution showed a smaller overall gain of ~6.2% (0.081° → 0.076°), but its strong dependence on transverse momentum leads to ~50–60% improvement at high momenta. Sharper azimuthal resolution enhances transverse momentum reconstruction, improves invariant-mass resolution of reconstructed particles, and reduces track overlap errors under high-occupancy conditions.

The tanλ **(dip angle)** resolution improved significantly by ~25%, decreasing from ~47.6 × 10^{-3} before the upgrade to ~35.9 × 10^{-3} after. Since tanλ defines the slope of tracks relative to the beam axis, this refinement improves 3D track fitting and enhances vertex resolution when combined with d_0 and z_0, especially for displaced decays.

The p_t **(transverse momentum)** resolution saw the largest relative improvement, from ~2.38% before to ~0.91% after—a gain of over 60%. Since momentum precision underpins invariant-mass reconstruction, missing-energy calculations, and kinematic fits, this dramatic improvement is vital for rare decay searches and new physics channels where small deviations in reconstructed momenta can mask or mimic new phenomena.

Summary Table of Resolution Improvements

Parameter	Before Upgrade	After Upgrade	Relative Improvement	Physics Impact
d_0 (Transverse IP)	~237 µm	~189 µm	~20.3%	Better vertex separation, improved secondary-vertex reconstruction, stronger flavor tagging
z_0 (Longitudinal IP)	~2711 µm	~2047 µm	~24.5%	More precise vertex separation along beam axis, critical for CP violation studies

ϕ_0 (Azimuthal Angle)	0.081°	0.076°	~6.2% global (~50–60% at high p_t)	Improved transverse momentum measurement, narrower invariant-mass peaks, reduced track overlap
tanλ (Dip Angle)	47.6×10^{-3}	35.9×10^{-3}	~25%	Sharper 3D track fitting, improved vertex extrapolation
p_t (Momentum)	2.38%	0.91%	~62%	Major gain in momentum precision, sharper invariant masses, better missing energy balance, rare decay sensitivity

Overall Effect on Belle II

The combined resolution improvements across all five parameters provide Belle II with a significantly enhanced tracking system. Sharper d_0 z_0, ϕ_0 $and\ tan\lambda$ allow more accurate vertex reconstruction, essential for distinguishing between B meson decays and background processes, as well as enabling time-dependent CP violation measurements with reduced uncertainty. The dramatic advance in p_t resolution further sharpens the precision of kinematic observables, directly benefiting searches for rare decays, invisible final states, and beyond-the-Standard-Model processes.

Taken together, these upgrades prepare Belle II to fully exploit SuperKEKB's unprecedented luminosity. The detector can now handle higher track multiplicities and background levels while delivering the precision needed to reduce both statistical and systematic uncertainties. Ultimately, this comprehensive performance improvement enhances Belle II's capacity to explore the flavor sector in detail, test the Standard Model to new limits, and provide sensitivity to new physics scenarios that may appear only in rare processes.

Acknowledgements

In completing this report, I would like to express my deepest gratitude to those who have guided and supported me throughout this journey. My heartfelt thanks go to **Dr. Nguyễn Anh Kỳ** for his invaluable guidance, patience, and encouragement, which provided me with the foundation and direction needed to complete this work. I am also sincerely grateful to **Dr. Đồng Thanh** for his insightful feedback and continuous support, which greatly enriched the quality of my research.

Without their mentorship and dedication, this report would not have been possible.

References

1. Abashian, A., et al. (Belle Collaboration). (2002). *The Belle Detector*. Nuclear Instruments and Methods in Physics Research Section A, 479(1), 117–232. https://doi.org/10.1016/S0168-9002(01)02013-7

2. Abe, T., Adachi, I., Ahn, B. S., Aihara, H., Akai, K., Aloisio, A., … & Zupanc, A. (2010). *Belle II Technical Design Report*. arXiv:1011.0352. https://arxiv.org/abs/1011.0352

3. Belle II Collaboration. (2022). *Belle II detector status and performance reports*. Belle II Internal Notes / Conference Contributions.

4. Belle II CDC Group. (2021). *Central Drift Chamber performance and issues in Run 2022*. Belle II Internal Report.

5. Belle II Collaboration. (n.d.). *Belle II detector overview diagrams and documentation*. Retrieved from Belle II official website.

6. Indico Belle II. (2019). *Belle II Central Drift Chamber electronics and gas system presentations*. KEK Indico. https://indico.belle2.org

7. IPNS. (2016, October). *Installation of the Belle II Central Drift Chamber completed*. KEK Institute of Particle and Nuclear Studies. https://www2.kek.jp/ipns/en/post/2016/10/belle2-cdc-installation/

8. Iwashita, T. (2014, July). *The Belle Central Drift Chamber*. Beauty 2014 Conference, Edinburgh, UK. CERN Indico. https://indico.cern.ch/event/308116/contributions/1679433/attachments/588051/809304/Beauty2014_iwashita_v4.pdf

9. Iwashita, T., Uno, S., Sumisawa, K., & Nakao, M. (2024, March). *Belle II CDC status and performance*. Belle II General Meeting, KEK, Japan. CERN Indico. https://indico.cern.ch/event/1408681/contributions/6122492/attachments/2947960/5181092/BelleII_CDC_UNO.pdf

10. Kuhr, T., Pulvermacher, C., Ritter, M., Hauth, T., & Braun, N. (2018). *The Belle II core software*. Computing and Software for Big Science, 3(1), 1–10. https://doi.org/10.1007/s41781-018-0017-9

11. Nishida, S., et al. (2017). *Time-of-Propagation (TOP) Counter for Belle II*. Nuclear Instruments and Methods in Physics Research A, 876, 100–103.

12. Taniguchi, N., et al. (2017). *Central Drift Chamber for Belle-II*. Journal of Instrumentation, 12(06), C06014. https://doi.org/10.1088/1748-0221/12/06/C06014

13. Tran, H. V. (2023). *Performance evaluation for the Belle II central drift chamber before long-shutdown 2022* (Master's internship report, University of Science and Technology of Hanoi).

14. Wikipedia. (2025). *Belle II Detector sub-detectors (ECL, KLM)*. Retrieved from https://en.wikipedia.org/wiki/Belle_II

15. Won, E., et al. (2018). *The Belle II Electromagnetic Calorimeter*. Nuclear Instruments and Methods in Physics Research A, 876, 96–99.